research articles Journal of proteome research

Panorganismal Gut Microbiome−Host Metabolic Crosstalk

Francois-Pierre J. Martin,*,†,‡ Norbert Sprenger,‡ Ivan K. S. Yap,† Yulan Wang,†,§ Rodrigo Bibiloni,‡ Florence Rochat,‡ Serge Rezzi,‡ Christine Cherbut,‡ Sunil Kochhar,‡ John C. Lindon,† Elaine Holmes,† and Jeremy K. Nicholson*,†

Department of Biomolecular Medicine, Division of Surgery, Oncology, Reproductive Biology and Anaesthetics, Faculty of Medicine, Imperial College London, Sir Alexander Fleming Building, South Kensington, London SW7 2AZ, United Kingdom, and Nestlé Research Center, P.O. Box 44, Vers-chez-les-Blanc, CH-1000 Lausanne 26, Switzerland

Received December 13, 2008

Coevolution shapes interorganismal crosstalk leading to profound and diverse cellular and metabolic changes as observed in gut dysbiosis in human diseases. Here, we modulated a simplified gut microbiota using pro-, pre-, and synbiotics to assess the depth of systemic metabolic exchanges in mice, using a multicompartmental modeling approach with metabolic signatures from 10 tissue/fluid compartments. The nutritionally induced microbial changes modulated host lipid, carbohydrate, and amino acid metabolism at a panorganismal scale. Galactosyl-oligosaccharides reduced lipogenesis, triacylglycerol incorporation into lipoproteins and triglyceride concentration in the liver and the kidney. Those changes were not correlated with decreased plasma lipoproteins that were specifically induced by *L. rhamnosus* supplementation. Additional alteration of transmethylation metabolic pathways (homocysteine-betaine) was observed in the liver and the pancreas following pre- and synbiotic microbial modulation, which may be of interest for control of glucose metabolism and insulin sensitivity. Probiotics also reduced hepatic glycogen and glutamine and adrenal ascorbate with inferred effects on energy homeostasis, antioxidation, and steroidogenesis. These studies show the breadth and the depth of gut microbiome modulations of host biochemistry and reveal that major mammalian metabolic processes are under symbiotic homeostatic control.

Keywords: human baby microbiota • metabonomics • prebiotics • probiotics • synbiotics

Introduction

All coelomate vertebrates and invertebrates have coevolved with symbiotic gut microbes that perform multiple digestive and metabolic functions[1] for the host, and this has resulted in the ability of organisms to engage in enhanced adaptive radiation to exploit new dietary resources. In man, dietary preferences, lifestyle and genetics influence microbial population and ecological development, and these interactions determine the health of both individuals and populations.[2,3] Perhaps one of the greatest challenges in modern biology is to interrogate and classify these critical transgenomic interactions and to understand their role in diverse human disease processes.

The consortium of symbiotic gut microorganisms (the microbiome) can be viewed as a metabolically adaptable, rapidly renewable and metabolically flexible virtual "organ".[4] It is well established that the gut microbiota plays an essential role in the development and homeostasis of the mucosal innate and adaptive immune system.[5] The maintenance of physiological equilibrium at the mucosal interface, on which both host and gut microbiota exert reciprocal control, is indeed determinant for metabolic health. Maybe not surprising, the nature of the gut microbiome−host interactions seems such that the host controls the microbiome community structure, a process that has evolved to attain specific benefits ranging from protection to nutrition to physiology.[6]

Besides direct control over the microbiota by the host, nutrition helps to shape the microbiota from birth onward. The gastrointestinal tract of a normal fetus is sterile *in utero* and is rapidly colonized with microbes from the mother at birth and subsequently from the surrounding environment, developing into a dense and complex microbial community.[7] Marked differences in gut microbiota composition of formula-fed and breast-fed neonates have been observed, and the nutritional composition of breast-milk as compared to formula milk is believed to be a key determinant to this end. Moreover, breastfeeding is associated with a lower incidence of infections, morbidity and mortality as compared to formula feeding,[8] and in part, this is thought to be due to the elevated bifidobacteria counts and the higher intestinal acidity[9] in breastfed infants.

* To whom correspondence should be addressed. Prof. J. Nicholson, E-mail: j.nicholson@imperial.ac.uk. Tel: +44 (0)20 7594 3195. Fax: +44 (0) 20 7594 3226. Dr. F−P. Martin, E-mail: francois-pierre.martin@rdls.nestle.com. Tel: + 41 (0) 21 785 8771. Fax: +41 (0) 21 785 9486.

† Imperial College London.

‡ Nestlé Research Center.

§ Present address: State Key Laboratory of Magnetic Resonance and Atomic and Molecular Physics, Wuhan Centre for Magnetic Resonance, Wuhan Institute of Physics and Mathematics, The Chinese Academy of Sciences, Wuhan, 430071, PR China.

10.1021/pr801068x CCC: $40.75

Published on Web 03/13/2009

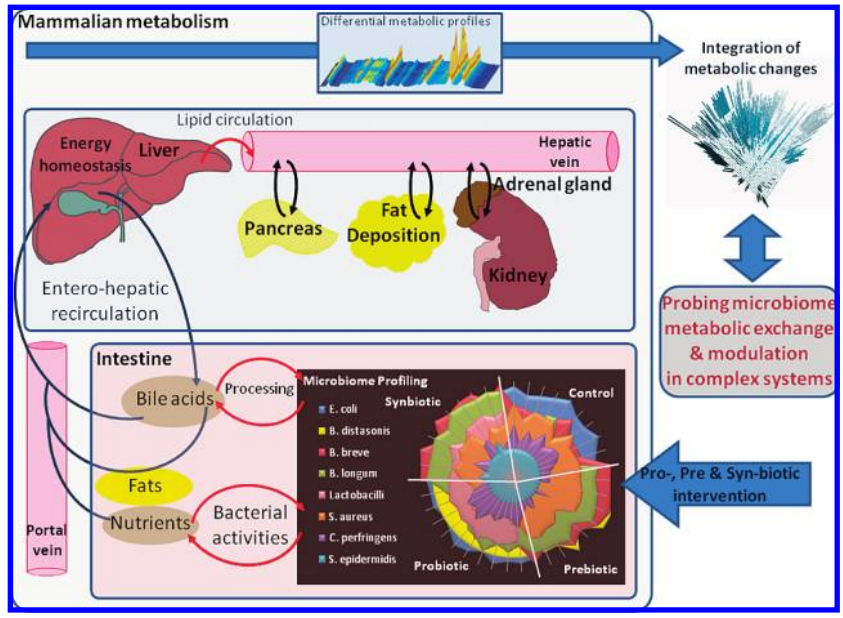

Figure 1. Metabolic effects of nutritional modulation of gut bacteria activities in a variety of different tissues underpinning the depth of symbiotic control. An analytical strategy based on the use of pro-, pre- and syn-biotic interventions enables the probing of microbiome symbiotic metabolic exchange and modulation in complex systems.

The acquired gut microbiota has subsequently profound effects on the determination of host nutrition, physiology, immunology and protective functions.[5,10,11] Increasingly, health disorders related to uncontrolled immune reactions and disequilibrated sugar and lipid metabolism are associated with changed gut microbiome community structures.[3,11,12] As the gut microbiota interacts strongly with the host and the ingested nutrients to determine immune and metabolic health as well as nutritional status, there is clearly an important role of understanding these interactions as part of optimized nutrition. Nutrimetabonomics provides a systems approach to assess systemic metabolic status of an individual, which encapsulates information on genetic and environmental factors, gut microbiota activity, lifestyle, and food habits.[2] These techniques have been used to decipher gut microbial-mammalian cometabolic processes linking host and symbiont physiology[13−15] and to assess the impact of nutritional interventions on microbial-mammalian cometabolism.[16,17] In particular, we reported that inoculating germfree mice with a model of human baby microbiota (HBM) was a well-adapted model to assess the impact of nutritional intervention on mammalian gut microbial metabolic interactions.[13] In addition, our results also demonstrated the limitations of the model in that HBM was not optimal for murine hosts because it drove the metabolism toward a prepathological state.[13]

Recently, we assessed the metabolic effects of *L. rhamnosus* probiotics and synbiotic supplementation with galactosyl-oligosaccharides on host system metabolism through the analysis of systemic biofluids and liver in gnotobiotic mice harboring HBM.[18,19] In the current work, we explored further the effects of single probiotics and prebiotics, and their combination (synbiotics), on the metabolic status of germfree mice during the establishment of the simplified HBM microbiota. To assess the underlying molecular mechanisms, we applied metabonomics to monitor the metabolism of major mammalian organs in combination with systemic biofluids, namely plasma, liver, urine, fecal extracts, pancreas, kidney cortex and medulla, adrenal gland extracts, cecal SCFAs, and ileal bile acids (Figure 1). This multicompartmental approach provides a way forward to assess the metabolic impact of dietary modulations of the gut microbiota at a panorganismal scale, i.e. at the level of every major biological compartment. Moreover, it helps the assessment of key functional relationships among various biological compartments, intercompartment metabolic contributions to overall host metabolism, and the identification of changes in interorgan cross-talk in relation to nutritional interventions.

Material and Methods

Animal Handling. This study was conducted under the appropriate national guidelines at the Nestlé Research Center (Lausanne, Switzerland). A total of 39 C3H female germfree mice (Charles River, France) were housed under the same environmental conditions and were fed with a standard semi-synthetic irradiated rodent diet.[20] At 8 weeks of age, the germfree mice received a single dose of human baby microbiota (HBM) bacteria mixture and were assigned randomly to 4 groups which followed different nutritional interventions over a 2 week period. Therefore, HBM was established simultaneously with the supplementations. One group was kept as control and was fed with a "basal mix" diet containing in composition 2.5% of a glucose-lactose mix (1.25% each) and received a saline drink *ad libitum* containing Man, Rogosa and Sharpe (MRS) culture medium ($n = 9$). A second group of mice was given daily *Lactobacillus rhamnosus* (NCC4007) at 10^8 bacteria in MRS per day mixed with the *ad libitum* saline solution and was fed with the "basal mix" diet (probiotic intervention, $n = 10$). A third group of mice was fed with a diet containing 3 g per 100 g diet of an in-house preparation of galacto-oligosaccharides and received an *ad libitum* saline drink containing MRS culture medium (prebiotic intervention, $n = 10$). A fourth group was given daily the *Lactobacillus rhamnosus* at 10^8 bacteria in MRS per day mixed with the *ad libitum* saline solution and was fed with the diet supplemented in prebiotics (synbiotic intervention, $n = 10$). Animals receiving

L. rhamnosus were grouped together in the same isolator to avoid cross-contaminations with other groups.

The in-house preparation of prebiotics is composed of 80% commercially available galactosyl-oligosaccharides (Vivinal-GOS, Borculo Domo Ingredients, The Netherlands)[21] and 20% of a mixture containing other galactosyl-oligosaccharide structures[19] (Supporting Information). The control diet was supplemented with lactose and glucose to control for the lactose and glucose that were brought into the experimental diets by the used galactosyl-oligosaccharide preparations.

The preparation of the HBM was previously described[18] (Supporting Information). A total of 7 bacteria were isolated, namely *Escherichia coli, Bifidobacterium breve* and *Bifidobacterium longum, Staphylococcus epidermidis* and *Staphylococcus aureus, Clostridium perfringens,* and *Bacteroides distasonis,* and they were mixed in equal amounts (approximatively 10^{10} cells/mL for each strain) for gavage. Bacterial cell mixtures were kept in frozen aliquots until use. *Lactobacillus rhamnosus* NCC4007, obtained from the Nestlé Culture Collection (Lausanne, Switzerland), was grown in MRS, concentrated and resuspended in fresh MRS to 4×10^9 CFU/mL. Aliquots of 1 mL were frozen, and each day, a fresh defrosted aliquot was introduced in the isolator and mixed with the saline drinking water.

Sample Collection. Two fecal pellets were collected in sterile conditions for microbial profiling and NMR spectroscopy. Morning spot urines were also sampled separately. Animals were weighed and then euthanized. Blood (400 μL) was collected into Li-heparin tubes and the plasma was obtained after centrifugation. Samples were frozen at −80 °C for NMR spectroscopy. The gastrointestinal tract from the duodenum to the cecum was removed from each animal. The cecal content was collected upon animal autopsy and snap-frozen immediately. The upper jejunum was retrieved in 10 mL sterile tubes containing 1 mL of glycerol for microbial profiling. Ileal flush samples were obtained by rinsing the ileal lumen with 1 mL of a phosphate buffer solution (0.2 M Na_2HPO_4/0.04 M NaH_2PO_4, pH = 7.4). A section of liver was sampled in the same lobe for each animal and snap-frozen. The pancreas and the two adrenal glands were also collected and snap-frozen for NMR spectroscopy. The kidneys were also dissected, and the cortex was separated from the medulla before being snap-frozen. Fluid and tissue samples were maintained at −80 °C prior to analysis.

Microbial Profiling of Fecal and Jejunal Contents and Bacterial Metabolic Activity. For fecal and jejunal samples, the bacterial populations for HBM and probiotics were determined using the conventional plating techniques reported previously[19] and described in the Supporting Information. Because bacterial populations were measured from the inoculation to euthanasia, the dilutions were defined at the beginning and kept constant throughout the study. However, the levels of certain bacteria dropped below the estimated range at the end of the study and the actual counts could not be obtained. Hence, we chose to use the less quantitative measures already given.

Total RNA was extracted from feces using a DNA/RNA Extraction kit (Qiagen, Switzerland). RNA integrity was assessed by electrophoresis of each sample in a 1.2% agarose gel that was stained with ethidium bromide solution and viewed by UV transillumination. RNA was quantified using the Ribogreen RNA Quantitation Reagent and Kit (Molecular Probes, Switzerland). Amplification of total bacterial community RNA was carried out by targeting 16S rRNA gene sequences with universal bacterial primers HDA1-GC and HDA-2 using the Qiagen OneStep RT-PCR kit (Qiagen, Switzerland) and a program comprising one cycle of 30 min at 50 °C (reverse transcription), one cycle of 15 min at 95 °C, and then 35 cycles of 30 s at 94 °C, 30 s at 56 °C, and 45 s at 72 °C. Fifty nanograms of RNA were used for each RT-PCR. The amplification products were checked by electrophoresis in a 2% agarose gel stained with ethidium bromide and viewed by UV transillumination prior to further analysis. Denaturing gradient gel electrophoresis (DGGE) was performed using a DCode apparatus (Bio-Rad, USA) and 6% polyacrylamide gels with a 30−55% gradient of 7 M urea and 40% (v/v) formamide that increased in the direction of electrophoresis. Electrophoretic runs were in TAE buffer (40 mM Tris, 20 mM acetic acid, 1 mM EDTA) at 130 V and 60 °C for 275 min. An identification ladder was prepared by extracting RNA from the individual components of the HBM used for gavage and then by RT-PCR amplification using the same pair of primers and amplification kit. Gels were stained with ethidium bromide solution for 20 min, washed with deionized water for 20 min, and viewed by UV transillumination. The intensity of staining of selected fragments in RNA-DGGE gel profiles was compared to that of *Escherichia coli* (which was constant in each sample and was used as an internal standard) and were analyzed from gel images with GeneTools gel analysis software (Syngene, Synoptics Ltd.).

Short Chain Fatty Acids and Lactate Cecal Content. Lactate was directly measured using a enzymatic BioAnalysis test kit (Boehringer Mannheim, R-Biopharm, Germany) according to the instructions provided by the manufacturer. Short chain fatty acids (SCFAs), that is, acetate, propionate, iso-butyrate, *n*-butyrate, iso-valerate and *n*-valerate, were extracted and measured as described previously and are reported in the Supporting Information.

^{1}H NMR Spectroscopic Analysis. Urine samples were prepared into 1.7 mm NMR tubes by mixing 20 μL of urine with 30 μL of phosphate buffer (pH 7.4) containing 90% D_2O as a field frequency lock and 0.05% sodium 3-(trimethylsilyl)propionate-2,2,3,3-d4 as a chemical shift reference. Plasma samples (100 μL) were introduced into a 5 mm NMR tube with 450 μL of saline solution containing 10% D_2O. Fecal pellets were homogenized in 650 μL of a phosphate buffer solution containing 90% D_2O and 0.05% TSP. The homogenates were sonicated at ambient temperature (298 K) for 30 min to destroy bacterial cells and then centrifuged at 6000*g* for 20 min. The supernatants were removed and centrifuged at 6000*g* for 10 min. Aliquots of 550 μL were then pipetted into 5 mm NMR tubes. Intact tissue samples of liver, pancreas, kidney cortex and medulla were bathed in ice cold saline D_2O solution. A portion of the tissue (∼15 mg) was packed into a zirconium oxide (ZrO_2) 4 mm outer diameter rotor. Due to the limited size of the adrenal glands, tissue extracts were prepared from both glands following the methods previously described.[22] Tissue samples were ground in 1 mL of acetonitrile/water (1:1). The supernatant containing the aqueous phase was collected, freeze-dried and redissolved in 60 μL of D_2O. Samples were spun for 10 min at 6000*g*, and 50 μL of the supernatant was then pipetted into 1.7 mm NMR tubes.

^{1}H NMR spectra were acquired for each sample using a Bruker DRX 600 NMR spectrometer (Bruker Biospin, Rheinstetten, Germany) operating at 600.13 MHz for ^{1}H observation. ^{1}H NMR spectra of plasma, urine, and extracts of adrenal gland and feces were acquired with a Bruker 5 mm TXI triple resonance probe at 298 K. ^{1}H NMR spectra of intact tissues of liver, pancreas, kidney cortex and medulla were acquired using

a standard Bruker high resolution MAS probe under magic-angle-spinning conditions at a spin rate of 5000 Hz.[22] Tissue samples were regulated at 283 K using cold N_2 gas to minimize any time-dependent biochemical degradation.

For all of the samples, a NMR spectrum was acquired using a standard one-dimensional pulse sequence with water suppression. In addition, for intact tissues and plasma samples, Carr-Purcell-Meiboom-Gill (CPMG) spin−echo spectra with water suppression were obtained. ^{1}H NMR spectra were acquired and processed according to the parameters previously published[18] and given in the Supporting Information.

UPLC−MS Material and Methods. Ultra Performance liquid chromatography (UPLC) of ileal flushes was performed on a ACQUITY UPLC system (Waters, Milford, MA) equipped with a Tof LCT-Premier (Waters MS Technologies, Manchester, UK) for mass detection using the method previously described[13] and is given in the Supporting Information.

Data Analysis. UPLC−MS data were processed using Micromass MarkerLynx Applications Manager Version 4.0 (Waters). The peaks of bile acids were identified by comparing the m/z ratio and retention time to the set of standard bile acids measured under the same conditions. Data were noise-reduced in both the UPLC and MS domains using a MarkerLynx standard routine. Integration of the UPLC−MS bile acid peaks was performed using ApexTrack2. Each peak integral was expressed as a percentage of the sum of integrals of the measured bile acids.

Statistical analysis of the changes in animal weights, bacterial populations, fecal composition in SCFAs and bile acid content in the feces and ileum was carried out using a two-tailed Mann−Whitney test.

The ^{1}H NMR spectra were digitized over the range of δ 0.2−10.0 using a Matlab script developed in-house (Imperial College London). The regions containing the water resonance (δ 4.5−5.2), and for urine spectra only the urea resonance (δ 4.5−6.2), were removed. The spectra were normalized to the sum of the spectrum prior to data analyses. O-PLS-DA of the NMR spectral data was carried out after applying scaling to unit variance.[23] The O-PLS-DA loading plots were processed according to the method described by Cloarec et al.[24] Here, the test for the significance of the Pearson product-moment correlation coefficient was used to calculate the cutoff value of the correlation coefficients at the level of $p < 0.05$. To test the validity of the model against overfitting, the cross-validation parameter Q^2 was computed and the standard 7-fold cross validation method was used.[24]

The statistical total correlation spectroscopy (STOCSY)[25] method was also applied to spectral peaks found to be significantly different between different nutritional interventions in order to elucidate the structure of metabolites and to establish possible associations with other metabolic components.

Hepatic Triglycerides Quantitation. Hepatic triglycerides were extracted, following lyophilisation of liver tissues, using a Folch extraction procedure.[26] Total triglycerides were hydrolyzed using an enzymatic kit (TG PAP 150, Biomérieux, France), and total glycerol concentration was determined by colorimetry.

Taqman Real-Time Polymerase Chain Reaction (PCR) Analysis of Hepatic Microsomal Triglyceride Transfer Protein (MTTP) and Fatty Acid Synthase (FAS). RNA extracted from frozen intact liver tissue was used for Taqman Real-Time PCR Analysis of MTTP and FAS. Briefly, RNA was extracted using TriPure Isolation Reagent (Roche, Switzerland) and purification with NucleoSpin RNA II kit (Macherey Nagel, Switzerland) according to the manufacturer's instructions. RNA purity and integrity were determined by RNA 6000 Nano LabChip Kit (Agilent Technologies, Switzerland). RNA quantification was achieved using RiboGreen RNA quantitation reagent kit. Total RNA from each sample was reverse transcribed with the first-strand cDNA synthesis kit for RT-PCR using ImProm-II Reverse Transcription System (Promega, Switzerland). TaqMan primers for MTTP and FAS (Applied Biosystems, Switzerland) were used together with Beta-2-microglobulin (B2M) as a house keeping gene. Real-time PCR amplification was performed using an ABI 7900HT Thermocycler (Applied Biosystems, Switzerland) with the following conditions: 2 min at 50 °C and 10 min at 95 °C for the initial setup, followed by 40 cycles at 95 °C for 15 s (denaturation) and 60 °C for 1 min (annealing and elongation). All samples were analyzed in triplicate. Relative gene expression was calculated after normalization to B2M.

Pixel Map Representation of the Intercompartments Metabolic Correlation. Correlation analysis was performed on normalized spectral intensities of metabolites discriminating the different groups according to nutritional intervention. To highlight major intra- and intercompartment metabolic correlations, the statistical analysis has been carried out only on metabolite extracts from urine, plasma, liver, pancreas and kidney cortex matrices. Pearson's correlation coefficients were generated when considering all the animals irrespectively of their group using a cutoff value of 0.5 for the absolute value of the coefficient $|r|$. Correlation coefficients above the cutoff are displayed using pixel maps. The value and the sign of the correlation were then color-coded (gradient of red colors for positive values, gradient of blue colors for negative values). The presence of colored pixels between specific metabolites reveals a correlation (above the cutoff) between these molecules that may reflect a functional association.

Results

Interventional Modulation of Transgenomic Metabolic Interactions and Microbiome Composition. Microbial analyses were performed on mouse stools and jejunum luminal contents to assess the effects of the nutritional interventions on the gut bacterial ecology of HBM-associated mice (Table 1). Daily consumption of *L. rhamnosus* resulted in increased colonization by *B. longum* in both the jejunum and feces compared to controls, and reduced fecal *S. aureus* populations. Prebiotic supplementation modified the intestinal microbial content with higher numbers of *B. breve, B. longum* and *Bacteroides distasonis* in both the jejunum and stools, while the *E. coli* and *C. perfringens* counts were decreased in the feces. Analysis of the samples obtained from HBM mice treated with the synbiotic mixture showed some effects on fecal microbiota that can be ascribed to additive or synergistic consequences of the single pro- and prebiotic intervention. The observed higher populations of *B. breve, B. longum* and lower numbers of *C. perfringens* were similar to those obtained when feeding the animals with prebiotics alone, while the reduction of *S. aureus* counts was similar to that induced with probiotics alone but of lower magnitude. The prebiotic-specific decrease in *E. coli* was not induced by the administration of synbiotic supplement. Denaturing gradient gel electrophoresis (DGGE) bands corresponding to *E. coli, B. longum* and *C. perfringens* showed appropriate resolution for analysis. For the 4 other strains, DGGE bands showed low intensity or were overlapped with each other (for *Bacteroides distasonis* and staphylococci). The

Table 1. Microbial Species Counts in Mouse Fecal and Jejunal Contents[a]

	bacterial counts/ groups	HBM ($n = 9$)	HBM + *L. rhamnosus* ($n = 10$)	HBM + prebiotic ($n = 10$)	HBM + symbiotic ($n = 10$)
Feces	*E. coli*	9.4 ± 0.3	9.3 ± 0.3	9.0 ± 0.2[c]	9.3 ± 0.2
	B. breve	8.1 ± 0.4	7.8 ± 0.4	9.8 ± 0.6[d]	9.7 ± 0.4[c]
	B. longum	6.7 ± 1.1	8.1 ± 0.6[c]	9.1 ± 0.3[d]	9.4 ± 0.2[d]
	C. perfringens	6.3 ± 0.5	6.5 ± 0.6	5.4 ± 0.7[c]	5.5 ± 0.5[c]
	S. epidermidis	<5	<5	<5	5.2 ± 0.3
	S. aureus	7.8 ± 0.5	6.1 ± 0.6[d]	7.8 ± 0.4	7.1 ± 0.4[c]
	Bacteroides distasonis	<7	<9	9.6 ± 1.2	<9
	L. rhamnosus	−	8.0 ± 0.2	−	7.8 ± 0.3
Jejunum	*E. coli*	3.8 ± 0.5	3.0 ± 1.0	4.1 ± 0.7	3.2 ± 0.8
	B. breve	2.3 ± 0.9	2.7 ± 0.9	3.9 ± 1.1[c]	3.5 ± 1.4[e]
	B. longum	<2	2.7 ± 1.0	3.9 ± 1.5	2.9 ± 1.3
	C. perfringens	2.8 ± 0.6	2.9 ± 0.6	2.4 ± 0.3	2.8 ± 0.3
	S. epidermidis	2.1 ± 0.3	<2	2.2 ± 0.4	2.0 ± 0.1
	S. aureus	3.6 ± 1.3	3.1 ± 0.8	4.9 ± 0.7[b]	3.2 ± 1.0
	Bacteroides distasonis	2.5 ± 1.0	3.1 ± 1.6	4.5 ± 1.4[c]	3.9 ± 1.7
	L. rhamnosus	−	2.7 ± 0.9	−	3.1 ± 1.2

[a] Log $_{10}$ of CFU (colony forming unit) given per gram of wet weight of feces or jejunal content. Data are presented as mean ± SD. The values for the groups receiving nutritional intervention were compared to the control HBM animals. [b] Designates significant difference at 95% confidence level. [c] Designates significant difference at 99% confidence level. [d] Designates significant difference at 99.9% confidence level. [e] Differences significant at 90% confidence level P-value = 0.094. – indicates that probiotics are not present in the gut microbiota.

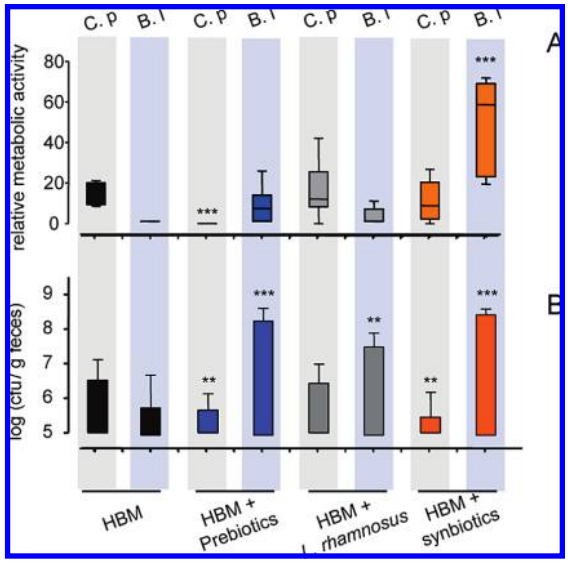

Figure 2. Relative metabolic activity and populations of resident *C. perfringens* and *B. longum* in feces. Relative metabolic activity with median and interquartile range (A) and Log_{10} of CFU (colony forming unit) given per gram of wet weight of feces with median and robust standard deviation (B) of resident *C. perfringens* (C.p) and *B. longum* (B.l). Represented are control HBM group (HBM, black, $n = 9$), group with prebiotics (HBM + prebiotic, blue, $n = 10$), group with *L. rhamnosus* probiotics (HBM + *L. rhamnosus*, grey, $n = 10$), and group with synbiotics *L. rhamnosus* in combination with prebiotics (HBM + *L. rhamnosus* + prebiotic, orange, $n = 10$). The values for the groups receiving nutritional intervention were compared to the control HBM animals. ** and *** designate significant differences at 99% and 99.9% confidence levels, respectively.

ratio of the band intensity of *B. longum* and *C. perfringens* to that of *E. coli* was calculated, and expressed as relative metabolic activity. Results were reported as medians in each group of mice together with the bacterial counts (Figure 2). The values for the groups receiving nutritional intervention were compared to the control HBM animals using a median Fisher-exact-test. Relative metabolic activity of *C. perfringens* was reduced by the prebiotic prior to the reduction of bacterial counts. The presence of probiotic or synbiotic had no significant effect on the relative metabolic activity of *C. perfringens* as compared to the controls. Comparing counts and relative metabolic activity of *B. longum* revealed an increased metabolic activity of *B. longum* in the synbiotic group as compared to the prebiotic group, although counts were equal between the two groups, and in the controls. These results indicate that while the overall colonization by *B. longum* is similar between the prebiotics alone and synbiotic fed animals, there is an increase in metabolic activity in the latter. In addition, statistical comparison of the individual animal body weights did not reveal any significant differences related to the different treatments (Table S1, Supporting Information).

Mutlicompartmental Metabolic Phenotyping and Microbiome Modulation. ^{1}H NMR spectroscopy was employed to analyze a range of biofluids[27] coupled with high resolution magic angle spinning NMR spectroscopic methods[28,29] to provide broad ranging metabolic phenotype profiles, that is, metabotypes,[14,30] across a range of compartments. Typical examples of ^{1}H spin−echo NMR spectra of plasma, intact liver, pancreas and kidney cortex tissues, and ^{1}H NMR spectra of adrenal glands, fecal extracts and urine from a HBM mouse supplemented with synbiotics are shown in Figure 3. Assignments of metabolites are given in Table 2 and discussed in the Supporting Information.

The metabolic changes in response to intervention were evaluated statistically using a series of O-PLS-DA models[23] to compare the ^{1}H NMR profiles of each treatment group with the control group, that is, using a series of pairwise comparisons. A statistically significant separation between controls and mice supplemented with pro-, pre- and synbiotics was observed for each biological matrix (blood plasma, urine, fecal extract, liver, pancreas, kidney cortex and medulla, and adrenal extract) as reflected by the high value of Q_Y^2, but no significant metabolic changes were observed in the pancreas of HBM mice supplemented with *L. rhamnosus* compared to the untreated HBM mice (Table 3). The major metabolites that contributed to group separation are given as area normalized intensities (means ± SD) in Table 3. Typical O-PLS-DA coefficients plots are presented for the pairwise comparison between HBM controls and HBM animals supplemented with the synbiotics

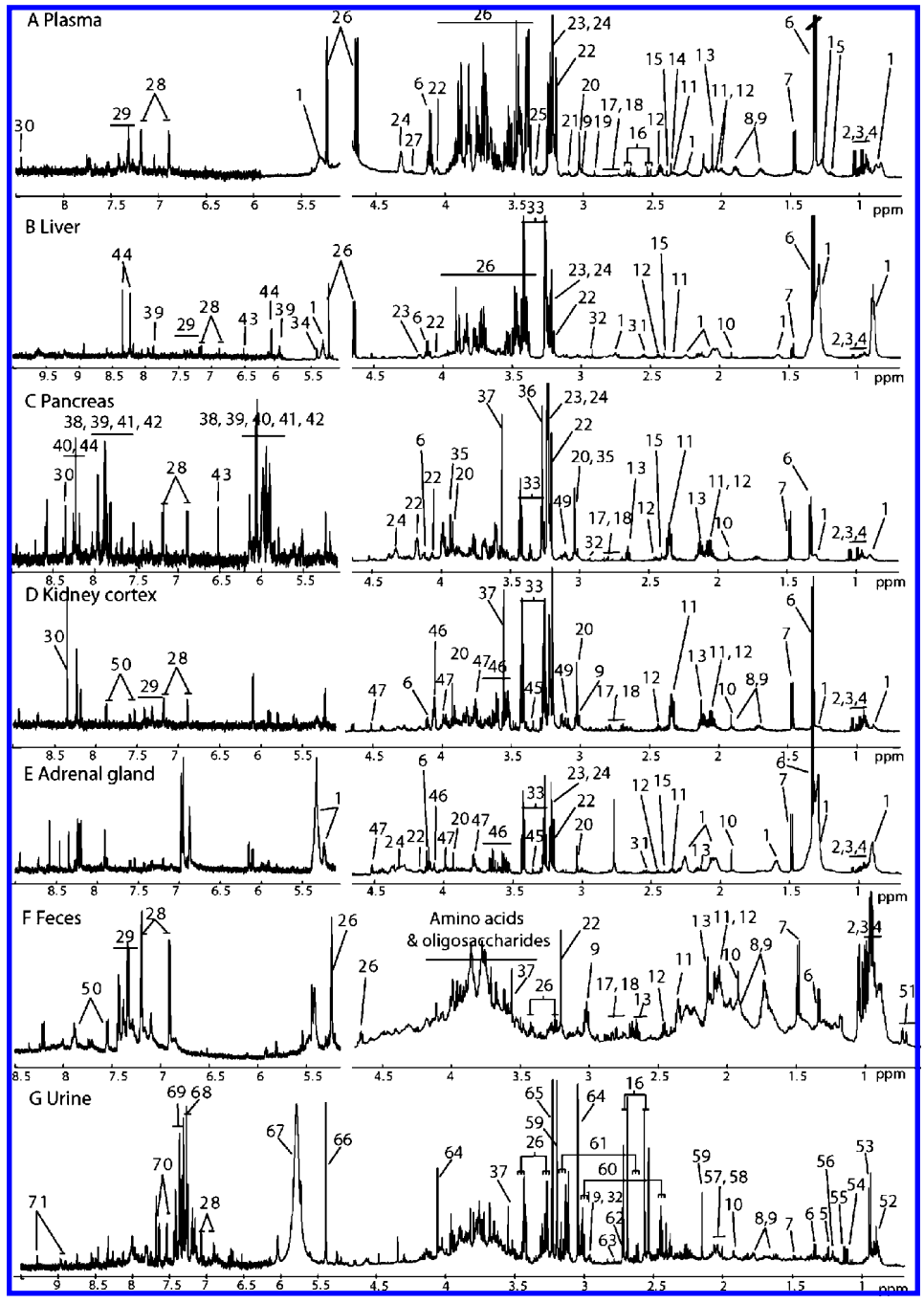

Figure 3. Typical 600 MHz ^{1}H NMR spectra of biofluids and intact tissues. Typical 600 MHz ^{1}H CPMG NMR spectra of plasma (A), intact liver (B), pancreas (C) and kidney cortex (D) tissues and ^{1}H NMR spectrum of adrenal glands extract (E), fecal extract (F) and urine (G) from a HBM mouse supplemented with synbiotics. The plasma regions δ 5.2−5.9 and 5.9−8.5 were magnified 2 and 6 times, respectively, compared to the aliphatic region (δ 0.7−4.5). The liver regions δ 5.2−5.8 and 5.8−10 were magnified 2 and 4 times, respectively. The pancreas and kidney cortex regions δ 5.18−9.0 were magnified 8 times. The spectra of the adrenal glands and fecal extracts were magnified 4 and 2 times, respectively, in the aromatic region (δ 5.2−8.5/9). The urine region 6.1−9.5 was magnified 4 times compared to the aliphatic region (δ 0.7−4.5). Key is given in Table 2.

in Figure 4 using back-scaling projection transformation.[24] The direction of the signals in the plots relative to zero indicates positive or negative covariance with the treated class compared to the controls. Each variable is color-coded according to its discriminating power as calculated from the correlation matrix, with variables highly influential in the discrimination highlighted in red (Figure 4).

Plasma Metabotypes. HBM mice fed with *L. rhamnosus* were distinguished from control HBM by significantly lower levels of plasma lipoproteins and choline (Table 3). Blood plasma of mice fed with the prebiotic showed a downward trend in glucose and increased levels of trimethylamine-*N*-oxide (TMAO), trimethylamine (TMA) and choline (Table 3). Mice supplemented with the synbiotic showed relative decreases in plasma lipoproteins and citrate, and relative increases in TMAO and TMA (Figure 4, Table 3).

Urinary Metabotypes. HBM mice receiving *L. rhamnosus* showed higher urinary excretion of α-keto-isovalerate and an

Table 2. Table of Assignment of the Metabolites in Biological Matrices

key	metabolites	moieties	δ ^{1}H (ppm) and multiplicity[a]
1	Lipids	CH_3, $(CH_2)n$, $CH_2-C=C$, $CH_2-C=O$, $=C-CH_2-C=$, $-CH=CH-$	0.89(m), 1.27(m), 2.0(m), 2.3(m), 2.78 (m), 5.3(m)
2	Isoleucine	αCH, βCH, γCH_3, δCH_3	3.65(d), 1.95(m), 0.99(t), 1.02(d)
3	Leucine	αCH, βCH_2, δCH_3, δCH_3	3.72(t), 1.96(m), 0.91(d), 0.94(d)
4	Valine	αCH, βCH, γCH_3	3.6(d), 2.26(m), 0.98(d), 1.04(d)
5	3-D-hydroxybutyrate	CH, CH2, γCH_3, CH_2	4.16(dt), 2.41(dd), 1.20(d), 2.31(dd)
6	Lactate	αCH, βCH_3	4.11(q), 1.32(d)
7	Alanine	αCH, βCH_3	3.77(q), 1.48(d)
8	Arginine	αCH, βCH_2, γCH_2, δCH_2	3.76(t), 1.89(m), 1.63(m), 3.23(t)
9	Lysine	αCH, βCH_2, γCH_2, δCH_2, ϵCH_2	3.77(t), 1.89(m), 1.72(m), 1.47(m), 3.01(t)
10	Acetate	CH_3	1.91(s)
11	Glutamate	αCH, βCH_2, γCH_2	3.75(m), 2.08(m), 2.34(m)
12	Glutamine	αCH, $\beta CH2$, γCH_2	3.77(m), 2.15(m), 2.44(m)
13	Methionine	αCH, βCH_2, $\gamma CH2$, δCH_3	3.78(m), 2.14(s), 2.6(dd), 2.13(s)
14	Succinate	CH_3	2.41(s)
15	Pyruvate	CH_3	2.37(s)
16	Citrate	half CH_2, half CH_2	2.55(d), 2.65 (d)
17	Aspartate	αCH, βCH_2	3.89(m), 2.68(m), 2.82 (m)
18	Asparagine	αCH, βCH_2	3.90(m), 2.86(m), 2.94(m)
19	Trimethylamine (TMA)	CH_3	2.87(s)
20	Creatine	N-CH_3, CH_2	3.03(s), 3.92(s)
21	Ethanolamine	CH_2OH, CH_2NH_2,	3.83(t), 3.15(t)
22	Choline	$N(CH_3)_3$, OCH_2, NCH_2	3.2(s), 4.05(t), 3.51(t)
23	Phosphorylcholine	$N(CH_3)_3$, OCH_2, NCH_2	3.22(s), 4.21(t), 3.61(t)
24	Glycerophosphocholine (GPC)	$N(CH_3)_3$, OCH_2, NCH_2	3.22(s), 4.32(t), 3.68(t)
25	Proline	αCH, βCH_2, γCH_2, δCH_2	4.11(t), 2.02(m)−2.33(m), 2.00(m), 3.34(t)
26	α-Glucose	H4, H2, H3, 1/2 CH2-C6, 1/2 CH2-C6, H5, H1	3.42 (t), 3.54 (dd), 3.71 (t), 3.72 (m), 3.76 (m), 3.83 (ddd), 5.23 (d)
26	β-Glucose	H2, H4, H5, H3, 1/2 CH2-C6, 1/2 CH2-C6, H1	3.24 (dd), 3.40 (t), 3.47 (ddd), 3.48 (t), 3.84 (m), 3.90 (dd), 4.64 (d)
27	Threonine	αCH, βCH_2, γCH_3	3.59(d), 4.25(m), 1.32(d)
28	Tyrosine	CH, CH	7.16(dd), 6.87(dd)
29	Phenylalanine	2,6-CH, 3,5-CH, 4-CH	7.40(m), 7.33(m), 7.35(m)
30	Formate	CH	8.45(s)
31	Glutathione	CH_2, CH_2, S-CH_2, N-CH, CH	2.17(m), 2.55(m), 2.95(m), 3.83(m), 4.56(m),
32	Dimethylglycine (DMG)	CH_2	2.93(s)
33	Taurine	N-CH_2, S-CH_2	3.26(t), 3.40(t)
34	Glycogen	Ring protons, 1-CH	3.35 − 4.0(m), 5.38 − 5.45(m)
35	Betaine	CH_2, CH_3	3.9(s), 3.27(s)
36	Trimethylamine-*N*-oxide (TMAO)	CH_3	3.26(s)
37	Glycine	CH_2	3.57(s)
38	Uracil	6-CH, 5-CH	7.54(d), 5.84(d)
39	Uridine	11-CH, 7-CH, 12-CH, 6-CH, 5-CH, 4-CH, half CH_2, half CH_2	7.88(d), 5.92(d), 5.9(d), 4.36(m), 4.24(t), 4.14(q), 3.92(dd), 3.81(dd)
40	Adenosine	14-CH, 8-CH, 1-CH, 2-CH, 3-CH, 4-CH, CH_2	8.32(s), 8.19(s), 6.05(d), 4.75(t), 4.48(dd), 4.34(m), 4.09(m)
41	Guanosine	14-CH, 1-CH, 2-CH, 3-CH, 4-CH, half CH_2, half CH_2	8.13(s), 5.94(d), 4.41(t), 4.24(q), 3.86(m)
42	Cytidine	12-CH, 11-CH, 1-CH, 2-CH, 3-CH, 4-CH, half CH_2, half CH_2	7.84(d), 6.06(d), 5.9(d), 4.30(m), 4.21(m), 4.12(m), 3.94(m), 3.82(m)
43	Fumarate	CH	6.53(s)
44	Inosine	14-CH, 8-CH, 1-CH, 4′-CH, 5′-CH, half CH_2, half CH_2	8.34(s), 8.22(s), 6.09(d), 4.76(t), 4.47(m), 4.28(q), 3.92(dd), 3.85(dd)
45	*Scyllo*-inositol	CH	3.34(s)
46	*Myo*-inositol	2-CH, 4,6-CH, 1,3-CH, 5-CH	4.06(t), 3.63(t), 3.53(dd), 3.29(t)
47	Ascorbate	CH, CH, half CH_2, half CH_2	4.52(d), 4.03(m), 3.76(d), 3.74(d)
48	Glycerol	2-CH, CH_2, CH_2	3.91 (m), 3.64(m), 3.56(m)
49	Cysteine	CH, half CH_2, half CH_2	3.97(t), 3.1(dd), 3.05(dd)
50	Tryptophan	4-CH, 7-CH, 2-CH, 5-CH, 6-CH, CH, half CH_2, half CH_2	7.74(d), 7.55(d), 7.33(s) 7.29(t), 7.21(t), 4.06(dd), 3.49(dd), 3.31(dd)
51	Bile acids	C-18 Methyl groups	
52	Butyrate	CH_3, CH_2, CH_2	0.90(t), 2.16(t), 1.56(m)
53	α-Keto-isocaproate	CH_3, CH, CH_2	0.94(d), 2.10(m), 2.61(d)
54	Isobutyrate	CH_3, CH	1.11(d), 3.02 (m)
55	α-Ketoisovalerate	CH_3, CH	1.13(d), 3.02(m)
56	3-Hydroxy-isovalerate	CH_3	1.21(s)

Table 2. Continued

key	metabolites	moieties	δ ^{1}H (ppm) and multiplicity[a]
57	*N*-acetyl-glycoproteins (Nac)	CH_3	2.04(s)
58	*O*-acetyl-glycoproteins	CH_3	2.08(s)
59	*N*-acetyl-carnitine	CH, N-CH_2, N-CH_3, Half CH_2COOH, Half CH_2COOH, O-CH_3,	3.85(m), 3.61(m), 3.19(s), 2.65(dd), 2.51(dd), 2.14 (s)
60	2-Oxoglutarate	CH_2, CH_2	3.01(t), 2.45(t)
61	β-Alanine	CH_2, CH_2	3.19(t), 2.56(t)
62	Dimethylamine	CH_3	2.72(s)
63	Sarcosine	CH_2, CH_3	3.61(s), 2.74(s)
64	Creatinine	CH_3, CH_2	3.06(s), 4.06(s)
65	Carnitine	N-CH_2, CH_3, CH_2COOH	3.43(m), 3.23(s), 2.44(dd)
66	Allantoin	CH	5.41(s)
67	Urea	NH_2	5.90(s)
68	*p*-Toluyl derivative (U2)	CH_3, CH_2, CH_2, CH_2	2.38(s), 7.31(d), 7.26(d), 5.42(m)
69	Phenylacetyl−glycine (PAG)	2,6-CH, 3,5-CH,7-CH, 10-CH	7.43(m), 7.37(m), 3.75(d), 3.68(s)
70	Indoleacetyl−glycine (IAG)	4-CH, 7-CH, 2-CH, 5-CH, 6-CH, CH_2, CH_2	7.64(d), 7.55(d), 7.35(s) 7.28(t), 7.19(t), 3.82(s), 3.73(s)
71	*N*-methylnicotinamide	2-CH, 6-CH, 4-CH, 5-CH, CH_3	9.28(s), 8.97(d), 8.90(d), 8.19(t), 4.48(s)
72	Isovalerate	CH_2, CH, CH_3	2.05(d), 1.94(m), 0.92(d)
73	α-Aminoadipate	CH, CH_2, half CH_2, half CH_2, CH_3	3.74(t), 2.25(t), 1.91(m) 1.84(m), 1.63(m)
74	Glycerate	CH, half CH_2, half CH_2,	4.09(m), 3.83(dd), 3.72(dd)

[a] Key: s, singlet; d, doublet; t, triplet; q, quartet; m, multiplet; dd, doublet of doublet.

upward trend in TMA levels, and lower levels of butyrate and isovalerate compared to controls (Table 3). Prebiotic supplementation affected the urinary metabolic profiles of HBM mice manifested by increased concentrations of carnitine, acetylcarnitine, taurine, and decreased concentrations of α-keto-isocaproate, butyrate, lysine, and α-aminoadipate (Table 3). The synbiotic supplementation caused similar changes to those observed with prebiotic alone with an additional increase in excretion of creatine and α-keto-isovalerate compared to controls (Figure 4, Table 3).

Fecal Metabotypes. Feeding HBM mice with *L. rhamnosus* resulted in higher fecal concentrations in several amino acids, including, valine, isoleucine, leucine, alanine, lysine, methionine, glutamine, glutamate, aspartate, asparagine, glycine, tyrosine, phenylalanine, tryptophan, and lactic acid (Table 3). Prebiotic supplementation showed marked effects on the metabolic profiles of fecal extracts of HBM mice that included relative increased concentrations in choline, acetate, glycine, oligosaccharides, and reduced levels of glucose and fatty acids (Table 3). Synbiotic supplementation induced increases in several amino acids, i.e. valine, leucine, isoleucine, alanine, glutamine, glutamate, glycine and choline, oligosaccharides, and decreased fecal fatty acids and glucose (Figure 4, Table 3).

Hepatic Metabotypes. The livers of mice fed with *L. rhamnosus* showed relative decreases in glycogen and fumarate (Table 3), whereas prebiotic supplemented mice showed relative decreases in hepatic triglycerides and relative increases in succinate, sarcosine, dimethylglycine (DMG), TMAO, betaine, choline, phosphocholine (PC), glucose, and alanine when compared to controls (Table 3). The metabolites that differentiated the liver of mice fed with synbiotics from control animals included a trend in decreased lipid and relative increases in succinate, sarcosine, DMG, TMA, dimethylamine (DMA), TMAO, betaine, choline, PC, and alanine (Figure 4, Table 3).

Pancreatic Metabotypes. Prebiotics and synbiotics affected the pancreas metabolic phenotypes of HBM mice, whereas probiotics alone did not induce statistically significant variations. The prebiotics-induced changes included increased levels of creatine, PC, TMAO, betaine and reduced levels of lactate, glycine and cysteine (Table 3). Consumption of synbiotics was correlated with relative higher levels of sarcosine, DMG, creatine, PC, TMAO, betaine and decreased concentrations of lactate, cysteine and threonine (Figure 4, Table 3).

Renal Cortical Metabotypes. HBM mice receiving *L. rhamnosus* showed increased concentrations of glutamine, lysine and TMA, and reduced levels of lipids and lactate in kidney cortex (Table 3). Consumption of prebiotics was correlated with a higher level of glutamine, and reduced concentrations of lipids compared to controls (Table 3). Feeding HBM mice with synbiotics led to increased concentrations of alanine, lysine, glutamine, glutamate, glycine, methionine, TMA and PC, and reduced concentrations of lipids and lactate (Figure 4, Table 3).

Renal Medullary Metabotypes. Probiotic supplementation induced changes in the kidney medulla as noted with a reduced level of hypotaurine and higher levels of alanine and TMAO compared to controls (Table 3). Feeding HBM mice with the prebiotic was correlated with a higher concentration of alanine and a reduced level of *myo*-inositol (Table 3). HBM mice that received synbiotic supplementation showed increased concentrations in alanine, glutamine and TMAO, and a lower level of hypotaurine (Figure 4, Table 3).

Adrenal Metabotypes. Adrenal glands obtained from HBM mice fed with *L. rhamnosus* showed higher levels of choline, glycerol, glycerate and decreases in ascorbate, aspartate, and asparagine (Table 3). Mice supplemented with the prebiotic showed increases in alanine, choline, glycerol, and glycerate and decreased ascorbate and aspartate (Table 3). The metabolites that differentiated mice fed with the synbiotic included increased alanine, glycerol, glycerate, choline, and decreased aspartate, asparagine and ascorbate (Figure 4, Table 3).

Cecal Short Chain Fatty Acids and Chiral Analysis of D/L Lactate. Significant reduction of lactate concentration was observed when feeding the HBM mice with the synbiotic mixture but not with other treatments (Table 4). The effect of the treatments on the cecal SCFA content is more complex. The acetate:propionate ratio was slightly decreased only in the probiotic treatment group (Table 4). Isobutyrate levels were unaffected by any treatments but *n*-butyrate was reduced by the probiotic treatment and further reduced by the prebiotic

Table 3. O-PLS-DA Model Summary for Pairwise Class Discrimination Using Data from NMR Spectra of Plasma, Urine, Adrenal Glands, Liver, Pancreas, Kidney Cortex and Medulla, and Feces[a]

metabolite	chemical shift and multiplicity[b]	HBM controls ($n = 9$)	HBM + *L. rhamnosus* ($n = 10$)	HBM + prebiotic ($n = 10$)	HBM + symbiotic ($n = 10$)
Adrenal glands			$Q_Y^2 = 48\%$, $R_X^2 = 30\%$	$Q_Y^2 = 36\%$, $R_X^2 = 33\%$	$Q_Y^2 = 79\%$, $R_X^2 = 37\%$
Alanine	1.48 (d)	1.8 ± 0.6	2.3 ± 0.6	2.4 ± 0.4[e]	2.6 ± 0.6[d]
Ascorbate	3.75 (m)	1.1 ± 0.3	0.7 ± 0.1[d]	1.0 ± 0.2	0.6 ± 0.2[d]
Aspartate	2.68 (m)	0.16 ± 0.03	0.13 ± 0.02[d]	0.14 ± 0.02	0.12 ± 0.02[e]
Asparagine	2.86 (m)	0.14 ± 0.02	0.12 ± 0.02[e]	0.12 ± 0.02[c]	0.1 ± 0.01[f]
Choline	3.56 (s)	1.5 ± 0.5	2.1 ± 0.4[d]	2.1 ± 0.4[d]	2.4 ± 0.4[f]
Glycerate	3.87 (m)	0.3 ± 0.04	0.4 ± 0.05[f]	0.4 ± 0.04[e]	0.5 ± 0.08[e]
Glycerol	3.65 (m)	0.7 ± 0.1	1.0 ± 0.3[e]	1.0 ± 0.2[d]	1.0 ± 0.2[f]
Lactate	1.32 (d)	5.6 ± 1.7	6.9 ± 0.9	7.3 ± 1.3	7.2 ± 0.9
U1	3.11 (s)	0.10 ± 0.02	0.09 ± 0.01	0.19 ± 0.03[f]	0.20 ± 0.02[f]
U2	3.13 (s)	0.12 ± 0.01	0.11 ± 0.01	0.16 ± 0.03[e]	0.16 ± 0.02[f]
Kidney medulla			$Q_Y^2 = 44\%$, $R_X^2 = 40\%$	$Q_Y^2 = 40\%$, $R_X^2 = 40\%$	$Q_Y^2 = 53\%$, $R_X^2 = 50\%$
Alanine	1.48 (d)	0.31 ± 0.07	0.57 ± 0.24[e]	0.43 ± 0.14[d]	0.65 ± 0.22[f]
Glutamine	2.44 (m)	0.07 ± 0.01	0.09 ± 0.03	0.08 ± 0.01	0.13 ± 0.02[f]
Hypotaurine	2.65 (t)	0.17 ± 0.03	0.09 ± 0.06[e]	0.14 ± 0.04	0.04 ± 0.02[f]
Myo-inositol	4.08 (m)	1.95 ± 0.18	1.95 ± 0.43	1.6 ± 0.31[d]	1.81 ± 0.27
TMAO	3.27 (s)	0.96 ± 0.28	1.59 ± 0.57[e]	1.1 ± 0.51	1.79 ± 0.58[e]
U2	3.13 (s)	0.15 ± 0.02	0.16 ± 0.07	0.51 ± 0.1[f]	0.47 ± 0.1[f]
U4	2.26 (m)	0.04 ± 0.01	0.05 ± 0.02	0.05 ± 0.01[e]	0.08 ± 0.02[f]
Kidney cortex			$Q_Y^2 = 35\%$, $R_X^2 = 32\%$	$Q_Y^2 = 28\%$, $R_X^2 = 30\%$	$Q_Y^2 = 72\%$, $R_X^2 = 36\%$
Alanine	1.48 (d)	0.75 ± 0.25	0.92 ± 0.39	0.75 ± 0.25	1.05 ± 0.18[d]
Glutamate	2.34 (m)	0.88 ± 0.11	0.89 ± 0.81	0.95 ± 0.31	1.10 ± 0.18[d]
Glutamine	2.44 (m)	0.07 ± 0.02	0.12 ± 0.04[e]	0.11 ± 0.02[e]	0.19 ± 0.03[f]
Glycine	3.57 (s)	3.83 ± 0.67	3.40 ± 1.46	3.59 ± 1.46	4.68 ± 1.12[c]
Lactate	1.32 (d)	4.10 ± 0.9	3.37 ± 0.75	3.36 ± 0.78	3.05 ± 0.60[d]
Lipids	1.27 (m)	1.49 ± 0.77	0.71 ± 0.33[d]	0.74 ± 0.39[d]	0.53 ± 0.30[e]
Lysine	1.72 (m)	0.10 ± 0.03	0.14 ± 0.04[d]	0.11 ± 0.03	0.17 ± 0.04[e]
Methionine	2.14 (s)	0.61 ± 0.15	0.77 ± 0.27	0.63 ± 0.17	1.02 ± 0.23[f]
PC	3.22 (s)	2.12 ± 0.27	2.45 ± 0.70	2.45 ± 0.56	3.6 ± 0.74[f]
TMA	2.91 (s)	0.02 ± 0.01	0.05 ± 0.02[e]	0.04 ± 0.03	0.09 ± 0.03[f]
U1	3.11 (s)	0.10 ± 0.04	0.21 ± 0.09[e]	0.28 ± 0.11[f]	0.38 ± 0.13[f]
U2	3.13 (s)	0.14 ± 0.02	0.25 ± 0.08[e]	0.35 ± 0.06[f]	0.10 ± 0.35[f]
U3	1.46 (s)	0.10 ± 0.01	0.14 ± 0.04[c]	0.28 ± 0.09[e]	0.39 ± 0.05[f]
U4	2.26 (m)	0.06 ± 0.02	0.09 ± 0.02[d]	0.07 ± 0.02	0.10 ± 0.02[f]
Pancreas			$Q_Y^2 < 0$	$Q_Y^2 = 10\%$, $R_X^2 = 37\%$	$Q_Y^2 = 46\%$, $R_X^2 = 26\%$
Betaine	3.90 (s)	1.22 ± 0.25	1.34 ± 0.18	1.65 ± 0.12[f]	1.71 ± 0.24[f]
Creatine	3.03 (s)	1.82 ± 0.56	1.92 ± 0.73	2.57 ± 0.99[c]	2.54 ± 0.92[d]
Cysteine	3.05 (dd)	0.38 ± 0.08	0.37 ± 0.14	0.28 ± 0.09[d]	0.24 ± 0.13[d]
DMG	2.93 (s)	0.03 ± 0.02	0.03 ± 0.02	0.04 ± 0.01[c]	0.08 ± 0.02[f]
Glycine	3.57 (s)	6.20 ± 1.93	5.75 ± 1.67	4.83 ± 1.28[c]	6.36 ± 1.55
Lactate	1.32 (d)	1.68 ± 0.44	1.67 ± 0.57	1.3 ± 0.36[d]	0.99 ± 0.25[f]
PC	3.23 (s)	16.85 ± 2.34	18.33 ± 1.58	19.38 ± 1.88[d]	20.12 ± 1.49[e]
Sarcosine	2.75 (s)	0.03 ± 0.03	0.03 ± 0.02	0.05 ± 0.02	0.05 ± 0.01[d]
Threonine	4.26 (m)	0.14 ± 0.04	0.15 ± 0.04	0.13 ± 0.02	0.12 ± 0.01
TMAO	3.27 (s)	2.62 ± 0.75	3.06 ± 0.78	4.17 ± 0.37[f]	4.53 ± 0.79[f]
Plasma			$Q_Y^2 = 15\%$, $R_X^2 = 86\%$	$Q_Y^2 = 29\%$, $R_X^2 = 86\%$	$Q_Y^2 = 81\%$, $R_X^2 = 85\%$
Choline	3.20 (s)	0.32 ± 0.06	0.24 ± 0.05[e]	0.5 ± 0.1[f]	0.42 ± 0.1[d]
Citrate	2.55 (d)	0.14 ± 0.04	0.12 ± 0.03	0.14 ± 0.04	0.08 ± 0.01[d]
Lipoproteins	0.85 (m)	0.5 ± 0.2	0.3 ± 0.1[d]	0.4 ± 0.1	0.3 ± 0.1[d]
TMA	2.87 (s)	0.06 ± 0.01	0.06 ± 0.1	0.09 ± 0.02[e]	0.1 ± 0.01[f]
TMAO	3.27 (s)	0.7 ± 0.16	0.86 ± 0.12[c]	1.1 ± 0.12[f]	1.1 ± 0.11[f]
U1	3.11 (s)	0.05 ± 0.01	0.04 ± 0.02	0.13 ± 0.02[f]	0.12 ± 0.02[f]
Liver			$Q_Y^2 = 31\%$, $R_X^2 = 31\%$	$Q_Y^2 = 36\%$, $R_X^2 = 46\%$	$Q_Y^2 = 72\%$, $R_X^2 = 49\%$
Alanine	1.46 (d)	0.29 ± 0.09	0.3 ± 0.1	0.4 ± 0.1[d]	0.4 ± 0.1[e]
Betaine	3.90 (s)	1.6 ± 0.3	1.5 ± 0.2	2.5 ± 0.2[f]	2.3 ± 0.3[f]
Choline	3.20 (s)	0.5 ± 0.2	0.6 ± 0.2	1.1 ± 0.2[f]	1.0 ± 0.3[f]
DMA	2.73 (s)	0.03 ± 0.01	0.05 ± 0.02	0.1 ± 0.02[f]	0.12 ± 0.03[f]
DMG	2.93 (s)	0.06 ± 0.02	0.09 ± 0.03[d]	0.19 ± 0.05[f]	0.22 ± 0.05[f]
Fumarate	6.52 (s)	0.03 ± 0.01	0.02 ± 0.01[f]	0.03 ± 0.0.02	0.03 ± 0.01
Gln	2.45 (m)	0.03 ± 0.01	0.03 ± 0.01	0.05 ± 0.01[f]	0.06 ± 0.01[f]
Glucose	4.64 (d)	2.4 ± 0.4	2.4 ± 0.5	2.9 ± 0.3[d]	2.6 ± 0.7
Glycogen	5.45 (m)	0.5 ± 0.1	0.3 ± 0.1[d]	0.5 ± 0.1	0.3 ± 0.1[c]

Table 3. Continued

metabolite	chemical shift and multiplicity[b]	HBM controls ($n = 9$)	HBM + *L. rhamnosus* ($n = 10$)	HBM + prebiotic ($n = 10$)	HBM + symbiotic ($n = 10$)
Lipids	1.27 (s)	3.6 ± 1.3	4.1 ± 1.1	2.1 ± 0.4[d]	2.5 ± 0.6[d]
PC	3.23 (s)	1.7 ± 0.3	1.7 ± 0.3	2.4 ± 0.3[f]	2.4 ± 0.2[f]
Sarcosine	2.75 (s)	0.14 ± 0.03	0.14 ± 0.03	0.18 ± 0.02[d]	0.22 ± 0.02[f]
Succinate	2.41 (s)	0.08 ± 0.03	0.09 ± 0.03	0.17 ± 0.09[d]	0.22 ± 0.1[e]
TMA	2.91 (s)	0.02 ± 0.01	0.02 ± 0.01	0.05 ± 0.01[f]	0.06 ± 0.02[f]
TMAO	3.27 (s)	1.7 ± 0.6	1.8 ± 0.4	4.4 ± 0.7[f]	4.9 ± 1.0[f]
U1	3.11 (s)	0.02 ± 0.01	0.04 ± 0.01[d]	0.08 ± 0.02[f]	0.09 ± 0.02[f]
U2	3.13 (s)	0.03 ± 0.02	0.04 ± 0.01	0.13 ± 0.03[f]	0.1 ± 0.04[f]
Feces			$Q_Y^2 = 50\%$, $R_X^2 = 37\%$	$Q_Y^2 = 96\%$, $R_X^2 = 50\%$	$Q_Y^2 = 95\%$, $R_X^2 = 57\%$
Acetate	1.91 (s)	0.62 ± 0.17	0.64 ± 0.18	1.0 ± 0.20[e]	0.93 ± 0.21[e]
Alanine	1.48 (d)	0.52 ± 0.07	0.69 ± 0.08[f]	0.66 ± 0.1[e]	0.71 ± 0.08[f]
Aspartate	2.68 (m)	0.11 ± 0.01	0.12 ± 0.01	0.09 ± 0.01	0.12 ± 0.01
Asparagine	2.86 (m)	0.10 ± 0.01	0.112 ± 0.01	0.10 ± 0.01	0.11 ± 0.01
Choline	3.19 (s)	1.0 ± 0.3	0.7 ± 0.3[c]	11.8 ± 2.2[f]	10.7 ± 2.6[f]
Fatty acids	0.87 (m)	0.52 ± 0.06	0.47 ± 0.06[c]	0.35 ± 0.02[f]	0.32 ± 0.03[f]
Glucose	5.23 (d)	0.14 ± 0.03	0.10 ± 0.03	0.07 ± 0.03[f]	0.06 ± 0.01[f]
Glutamate	2.34 (m)	0.31 ± 0.02	0.38 ± 0.07[d]	0.34 ± 0.05	0.40 ± 0.03[f]
Glutamine	2.44 (m)	0.13 ± 0.02	0.15 ± 0.03[d]	0.17 ± 0.1[f]	0.18 ± 0.01[f]
Glycine	3.57 (s)	0.42 ± 0.1	0.54 ± 0.06[d]	0.62 ± 0.08[f]	0.61 ± 0.09[e]
Isoleucine	0.96 (t)	0.39 ± 0.04	0.50 ± 0.08[e]	0.48 ± 0.08[e]	0.51 ± 0.06[f]
Lactate	1.33 (d)	0.49 ± 0.06	0.53 ± 0.07	0.52 ± 0.07	0.54 ± 0.09
Leucine	1.01 (d)	0.46 ± 0.06	0.56 ± 0.07[e]	0.52 ± 0.07[c]	0.58 ± 0.05[f]
Lysine	1.78 (m)	0.44 ± 0.03	0.49 ± 0.04[d]	0.37 ± 0.04[f]	0.40 ± 0.04[d]
Methionine	2.14 (s)	0.46 ± 0.05	0.55 ± 0.09[d]	0.49 ± 0.06	0.52 ± 0.03[e]
Oligosaccharides O1	3.88 (m)	0.46 ± 0.03	0.46 ± 0.07	0.77 ± 0.05[f]	0.77 ± 0.05[f]
Phenylalanine	7.40 (m)	0.02 ± 0.01	0.03 ± 0.01[e]	0.03 ± 0.01[e]	0.04 ± 0.01[f]
Tryptophane	7.51 (d)	0.02 ± 0.001	0.03 ± 0.01[c]	0.03 ± 0.01	0.04 ± 0.01[f]
Tyrosine	7.20 (d)	0.06 ± 0.01	0.08 ± 0.02[d]	0.07 ± 0.01	0.08 ± 0.01[d]
U1	3.11 (s)	0.11 ± 0.01	0.12 ± 0.01	0.25 ± 0.04[f]	0.23 ± 0.03[f]
U2	3.13 (s)	0.10 ± 0.01	0.10 ± 0.01	0.25 ± 0.04[f]	0.22 ± 0.05[f]
Valine	1.04 (d)	0.47 ± 0.07	0.60 ± 0.07[f]	0.57 ± 0.06[e]	0.63 ± 0.06[f]
Urine			$Q_Y^2 = 45\%$, $R_X^2 = 48\%$	$Q_Y^2 = 70\%$, $R_X^2 = 49\%$	$Q_Y^2 = 78\%$, $R_X^2 = 52\%$
Butyrate	0.90 (t)	0.5 ± 0.1	0.4 ± 0.1[d]	0.3 ± 0.1[e]	0.4 ± 0.08[e]
Carnitine	3.23 (s)	0.3 ± 0.06	0.32 ± 0.09	5.2 ± 1.3[f]	5.2 ± 1.3[f]
Creatine	3.92 (s)	0.48 ± 0.2	0.66 ± 0.4	0.65 ± 0.5	1.17 ± 0.9[d]
Lysine	1.78 (m)	0.42 ± 0.04	0.41 ± 0.12	0.25 ± 0.04[f]	0.27 ± 0.01[f]
N-acetyl-carnitine	3.19 (s)	0.17 ± 0.02	0.17 ± 0.02	1.3 ± 0.3[f]	1.2 ± 0.4[f]
Taurine	3.44 (t)	1.94 ± 0.91	1.37 ± 1.07	2.02 ± 0.92	2.28 ± 1.06
TMA	2.91 (m)	0.12 ± 0.03	0.17 ± 0.07	0.12 ± 0.04	0.26 ± 0.14
Isovalerate	0.92 (d)	0.19 ± 0.06	0.14 ± 0.04[d]	0.17 ± 0.03	0.12 ± 0.02[e]
α-keto-isocaproate	0.94 (d)	1.3 ± 0.3	1.1 ± 0.3	0.9 ± 0.1[d]	0.9 ± 0.2[d]
α-keto-isovalerate	1.14 (d)	0.19 ± 0.03	0.27 ± 0.1[d]	0.18 ± 0.04	0.25 ± 0.04[d]
α-aminoadipate	2.32 (m)	0.33 ± 0.05	0.23 ± 0.06[e]	0.19 ± 0.02[f]	0.19 ± 0.03[f]

[a] O-PLS models were generated with 1 predictive component, and 2 orthogonal components to discriminate between 2 groups of mice. The R_X^2 value shows how much of the variation in the dataset X is explained by the model. The Q_Y^2 value represents the predictability of the models, and relates to its statistical validity. Data are presented as area normalized intensities (a.u.) of representative metabolite signals as means ± standard deviation (SD). The values for the HBM mice supplemented with pro-, pre-, and synbiotics were compared to HBM control mice. [b] Key: s, singlet; d, doublet; t, triplet; q, quartet; m, multiplet. [c] Designates significant difference at 90% confidence level. [d] Designates significant difference at 95% confidence level. [e] Designates significant difference at 99% confidence level. [f] Designates significant difference at 99.9% confidence level.

administration, while coadministration did not result in any synergistic enhancements of changes. For isovalerate, the probiotic, the prebiotic and the synbiotic supplementations caused a similar increase. *n*-Valerate was reduced by the prebiotic supplement and the synbiotic treatment induced the same changes as the prebiotic.

UPLC-MS Analysis of Bile Acid Metabolites in Ileal Flushes. The proportion of bile acids in ileal flushes from the different groups is given as mean ± SD of the percentage of the total bile acid content of each biological matrix (Table 5). Taurochenodeoxycholic acid (TCDCA) was reduced in prebiotic and synbiotic supplemented mice but not in mice receiving the probiotic. The synbiotic treatment had less effect than prebiotics alone as observed with small reductions in tauroursodeoxycholic acid (TUDCA) in prebiotic treated mice. Moreover, the ileal profiles of probiotic supplemented mice showed a decrease in tauro-beta-muricholic acid (TβMCA) and an increase in taurocholic acid (TCA).

Intra- and Intercompartmental Metabolite Correlation Analysis. To summarize and highlight major intra- and intercompartmental metabolic correlations suggested by pairwise statistical analyses, a correlation analysis was performed to identify any latent metabolic links between urine, plasma, liver, pancreas and kidney cortex biological matrices (Figure 5A). Such analyses were generated when considering all the animals irrespectively of their group. Noticeably, these analyses highlighted the strong correlation between metabolites involved in choline, methylamine, betaine and homocysteine metabolism.

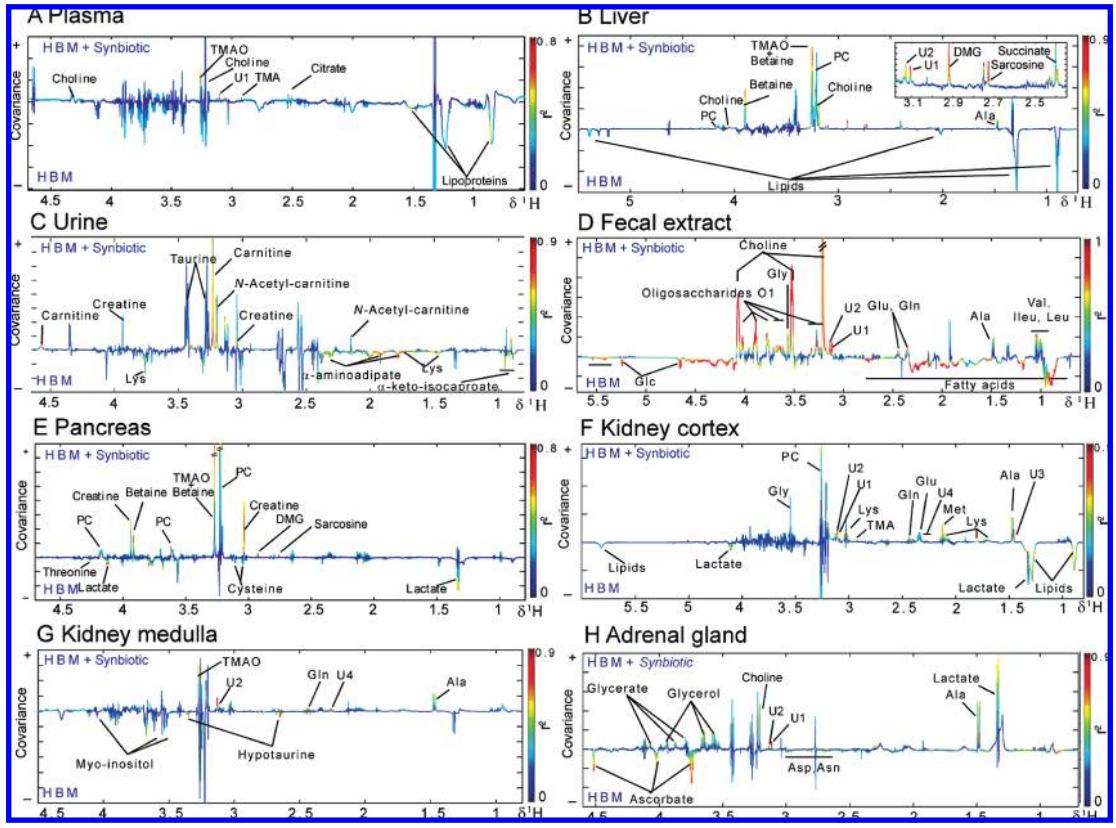

Figure 4. O-PLS-DA coefficients plots for the models discriminating the control HBM mice (negative) and the animals fed with synbiotics (positive) derived from O-PLS-DA of ^{1}H NMR spectra of plasma (A), liver (B), urine (C), fecal extract (D), pancreas (E), kidney cortex (F) and medulla (G), and adrenal glands (H).

Table 4. Lactate and Short Chain Fatty Acid Cecal Content[a]

SCFA concentration	HBM controls ($n = 9$)	HBM + *L. rhamnosus* ($n = 10$)	HBM + prebiotic ($n = 10$)	HBM + symbiotic ($n = 10$)
D-Lactate	3.3 ± 1.2	2.2 ± 1.8	3.1 ± 1.43	1.5 ± 0.9[b]
L-Lactate	4.1 ± 1.1	4.1 ± 1.8	4.3 ± 1.5	3.0 ± 0.8[e]
Acetate	70.5 ± 1.9	68.3 ± 2.0[b]	69.8 ± 2.5	71.7 ± 5
Propionate	18.9 ± 2.1	21.3 ± 2.2[b]	20.9 ± 3	19.1 ± 2.5
Isobutyrate	1.1 ± 0.2	1.2 ± 0.2	1.3 ± 0.2	1.2 ± 0.3
Butyrate	6.4 ± 2.7	5.3 ± 0.3[b]	4.2 ± 0.7[d]	4.0 ± 1.1[d]
Isovalerate	2.2 ± 0.6	3.2 ± 0.9[b]	3.2 ± 1.0[b]	3.3 ± 1.3[b]
Valerate	0.9 ± 0.2	0.8 ± 0.3	0.6 ± 0.2[c]	0.6 ± 0.2[b]

[a] Lactate concentrations are given in mg/100 mg of total content of dry feces and are presented as means ± standard deviation (SD). SCFAs data are given in relative concentrations of total dry fecal content in SCFAs and are presented as means ± SD. The values for the groups receiving nutritional intervention were compared to the control HBM animals. [b] Designates significant difference at 95% confidence level. [c] Designates significant difference at 99% confidence level. [d] Designates significant difference at 99.9% confidence level. [e] Difference significant at 90% confidence level P-value = 0.064.

Table 5. Bile Acid Composition in Ileal Flushes[a]

Microbiota/Bile acids	HBM controls ($n = 9$)	HBM + *L. rhamnosus* ($n = 10$)	HBM + prebiotic ($n = 10$)	HBM + symbiotic ($n = 10$)
CA	0.1 ± 0.1	0.1 ± 0.1	0.3 ± 0.8	0.1 ± 0.1
βMCA	0.1 ± 0.1	0.1 ± 0.1	0.1 ± 0.1	0.1 ± 0.1
TCDCA	0.8 ± 0.5	1.1 ± 0.5	0.2 ± 0.4[b]	0.6 ± 0.3[b]
TDCA	0.5 ± 0.1	0.1 ± 0.3	0.1 ± 0.1	0.2 ± 0.1
TUDCA	2.3 ± 1.8	2.8 ± 1.6	0.8 ± 1.2[b]	2.0 ± 1.1
TβMCA	73.0 ± 13.6	60.6 ± 11.7[b]	71.3 ± 14.9	75.7 ± 11.5
TCA	23.3 ± 14.0	35.3 ± 11.7[b]	27.3 ± 14.5	21.5 ± 11.3

[a] Relative composition in bile acids given in relative concentrations of total bile acid content. Data are presented as means ± standard deviation (SD). The key is given in UPLC-MS material and methods. The values for the groups receiving nutritional intervention were compared to the control HBM animals. [b] Designates significant difference at a 95% confidence level.

This is illustrated with positive correlations between the urinary excretions of carnitine and *N*-acetyl-carnitine, plasma and liver levels of choline, TMA and TMAO, hepatic concentrations of PC, betaine, DMG, sarcosine, pancreatic betaine, PC, TMAO and kidney content in phosphocholine. Interestingly, pixel maps also indicated a negative correlation between hepatic lipids and urinary excretion of carnitine, and *N*-acetyl-carnitine, plasma choline, and liver concentration of TMA, TMAO, DMG,

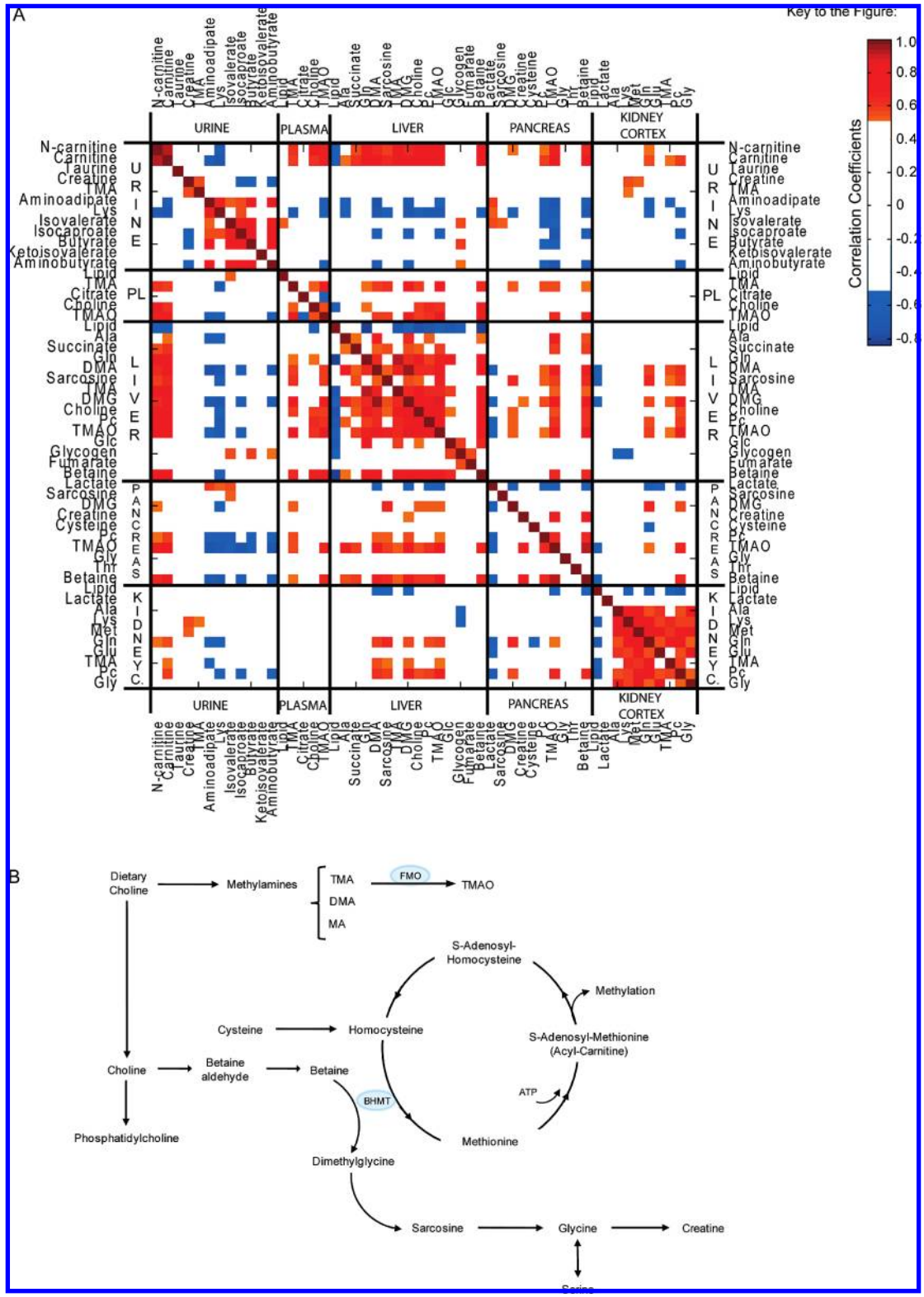

Figure 5. (A) Pixel mapping highlights of major intra- and intercompartment metabolic correlations. Correlation analysis was performed on metabolites discriminating the different groups in urine, plasma, liver, pancreas and kidney cortex. The cutoff value of 0.5 was applied to the absolute value of the coefficient |r| for displaying the correlations between metabolites. Correlation values are displayed as a color-coded pixel map according to correlation value (gradient of red colors for positive values, gradient of blue colors for negative values). (B) Schematic representation of methyl transfer in betaine and methionine metabolism. Key: Ala, alanine; ATP, Adenosine triphosphate; BHMT, Betaine-homocysteine methyl transferase; DMA, dimethylamine; DMG, dimethylglycine; Glc, glucose; Gln, glutamine; Glu, glutamate; Gly, glycine; FMO, flavine monooxygenase; Lys, lysine; MA, methylamine; Met, methionine; *Pc*, phosphocholine; Thr, threonine; TMA, trimethylamine; TMAO, trimethylamine-*N*-oxide. Biological compartments are coded "Pl", plasma, and "Kidney C.", kidney cortex.

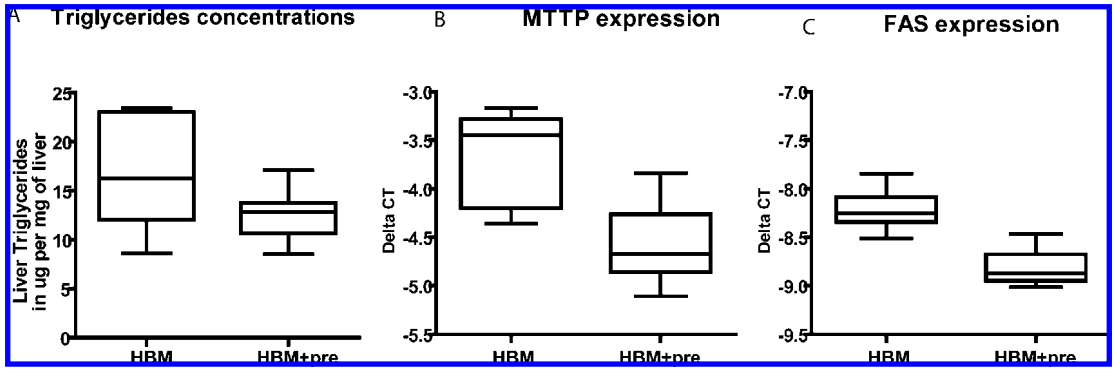

Figure 6. (A) Comparison of the concentrations of triglycerides in the liver of HBM controls ($n = 9$) and HBM mice supplemented with prebiotics ($n = 9$) displayed using box-and-whisker plots. Groups were compared using unpaired Student's *t*-test and the difference was statistical significant at 95% confidence level. Comparison of the expression of (B) microsomal triglyceride transfer protein (MTTP) and (C) fatty acid synthase (FAS) in the liver of HBM controls ($n = 9$) and HBM mice supplemented with prebiotics ($n = 9$). Differences between the groups are displayed using box-and-whisker plots. The decrease in expression levels in HBM + prebiotics animals was significant at 99.9% confidence level when using unpaired Student's *t*-test. Key: Delta CT is the difference between the threshold cycle of the gene of interest and that of the endogeneous reference gene.

choline, PC, betaine, DMG, sarcosine, but also glucose and glycogen. Moreover, correlation analysis indicated that the levels of kidney lipids are negatively correlated with liver concentrations in DMG, DMA and sarcosine, pancreas levels of TMAO and betaine, kidney cortex content in TMA, PC, glutamine and lysine.

Discussion

Application of multicompartmental metabolic profiling here demonstrates the extent of the functional relationship between gut microbiome modulation and the metabolite composition of 10 biological matrices that link to host metabolic health. The metabolic effects of *L. rhamnosus* given alone or as synbiotics to germfree mice simultaneously colonized with HBM were similar to those previously observed in gnotobiotic mice harboring HBM.[19] Our data also suggest that major mammalian metabolic processes are under gut symbiont homeostatic control, and that galactosyl-oligosaccharides supplementation alone or as synbiotics might have profound implications for maintenance of metabolic health.

Prebiotic Modulation of Gut Microbiota. Complementary to our previous studies on probiotics and synbiotics,[18,19] we assessed the effects of single prebiotic intervention in HBM mice. Galactosyl-oligosaccharides increased the populations of *B. breve* and *B. longum*, which are reported to digest galactosyl-oligosaccharides through specific β-galactosidases.[31−33] In particular, *Bifidobacteria* have shown a high capacity to metabolize dietary oligosaccharides into large quantities of SCFAs,[34] as observed here with increased levels of acetate in the feces. Moreover, the acidification of the luminal environment resulting of the fermentation of carbohydrates by bifidobacteria may contribute to the reduced *C. perfringens* and *E. coli* populations.[33,35] However, the marked reduction of the cecal butyrate content with prebiotics correlates with the reduction of *C. perfringens*, which is a primary butyrate producer.

Prebiotic Nutritional Intervention Links to Different Hepatic and Pancreatic Betaine-Homocysteine Metabolism. We observed altered transmethylation metabolic pathways that closely interconnect phosphocholine, betaine, dimethylgycine, sarcosine, choline, betaine and the formation of methionine from homocysteine,[36] in liver and pancreas. As a methyl donor, betaine is catabolized to dimethylglycine *via* the enzyme betaine-homocysteine-methyltransferase (BHMT), primarily in the liver and kidneys, and secondarily in the pancreas as summarized in Figure 5-B.[37,38] The coupled conversion of homocysteine to methionine is crucial for maintaining methionine homeostasis, detoxifying homocysteine, and producing *S*-adenosylmethionine.[37] The relative increased concentrations of hepatic and pancreatic phosphocholine, betaine, dimethylgycine, sarcosine and choline in the liver suggested higher betaine synthesis from choline and stimulated transmethylation in the methionine cycle, as evidenced in the pancreas by the observed reduced levels of cysteine. This hypothesis is in agreement with reports of compensatory changes between these metabolic pathways.[36,38,39] Moreover, betaine homocysteine metabolism is directly involved in the synthesis of phospholipids and carnitine.[37,40] Higher urinary excretions of carnitine and acetyl-carnitine bring additional evidence of a stimulation of these biochemical processes.[41,42]

Prebiotic Supplementation Induced a Different Lipid Metabolism in Liver and Kidney. Our metabonomic analyses revealed that prebiotics alone induced a significant reduction of lipids in the liver compared to controls, whereas no alterations of blood plasma lipoproteins were observed. Likely, these hepatic changes are in triglycerides, which are the major source of lipids in the liver. Dietary oligosaccharides may reduce hepatic lipids through a modulation of hepatic lipogenic enzyme activities, postprandial insulinemia and glycemia.[43] We have here measured the concentration of triglycerides, and the gene expression of microsomal triglyceride transfer protein (MTTP) and fatty acid synthase (FAS) in the liver of controls and mice supplemented with prebiotics. Our results confirmed that galactosyl-oligossachrides decreased hepatic triglycerides, a metabolic event associated with decreased lipogenesis (reduced FAS expression) and reduced incorporation of triacylglycerols into nascent lipoprotein particles (reduced MTTP expression) (Figure 6). Metabonomic analysis of kidney tissues revealed an additional reduction of its content in lipids. The kidney contributes to lipid metabolism through the uptake and β-oxidation of long-chain fatty acids from the blood stream,[44] the uptake of protein-bound lipids and its ability to express apolipoproteins.[45] Therefore, the observed multiorgan metabolic changes showed the importance of galactosyl-oligosaccharides in modulating system lipid metabolism.

The implications of our findings on lipid synthesis, circulation, and deposition must be investigated further in relation with the betaine-homocysteine metabolism. Indeed, increased BHMT metabolism is a potential mechanism contributing to higher ApoB secretion available for VLDL assembly.[46] Previous studies show complex carbohydrate diets result in higher secretion of nascent VLDL particles, smaller in size and carrying less triacylglycerols, and increased VLDL apo B fractional catabolic rates.[47] Therefore, our observation of enhanced BHMT metabolism and lower MTTP expression indicates higher apo B apoproteins synthesis and decreased transfer of lipids into nascent lipoproteins, which suggests the involvement of a similar mechanism in response to prebiotic interventions. Our observation may be of importance with the discovery that homocysteine may play a role in insulin release mechanism and pancreatic β-cell function in diabetes.[48] Recently, prebiotic stimulation of bifidobacteria was also correlated with improved glucose tolerance and glucose-induced insulin secretion.[49,50]

Probiotic Supplementation Modulates Gut Microbial Mammalian Cometabolism. In the current experiment, *L. rhamnosus* supplementation resulted in a specific increased population of *B. longum* and decreased counts of *S. aureus*, as previously observed.[18] Multicompartmental metabonomics revealed that probiotic metabolic effects were also reproducible in this design of experiment, as noted with reduced plasma lipoproteins and hepatic levels of glutamine and glycogen.[18] The novel application of metabonomics to monitor adrenal gland metabolic variations revealed a correlated reduction in its content of ascorbate. The adrenal gland is among the organs with the highest concentration of ascorbate in the body, a crucial cofactor for catecholamine biosynthesis, antioxidation and adrenal steroidogenesis.[51,52] Since ascorbate is crucial to the control of adrenal catecholamine levels, the observed changes in lipoproteins and gluconeogenetic pathways may be associated to the gut microbial modulation of the adrenal pool of ascorbate.[53] Further work is needed to decipher the mechanism of action of probiotics and their functional implications.

Synbiotic-Specific Host and Bacterial Cometabolism. Overall, synbiotic nutritional intervention resulted in complementary effects of pro- and prebiotics, at both bacterial and host metabolic levels (Tables 1, 3 and 4). However, the combination of galactosyl-oligosaccharides and *L. rhamnosus* induced a more significant bifidobacteria growth, and increased *B. longum* metabolic activity (Figure 2). The ability of *B. longum* to utilize galacto-oligosaccharides extensively[54,55] is dependent on the pattern of glycosidic linkages and thus on the existence of specific β-galactosidases.[56] Our observations suggest a synergistic interaction whereby *L. rhamnosus* may extend the *B. longum* metabolic capacities to degrade oligosaccharides. However, synbiotic supplementation had minimal effects on bacterial production of SCFAs in the cecum (Table 4) and the feces (Table 3) when compared to prebiotics alone. At the level of host cell pathways, synbiotic supplementation reduced levels of plasma lipoproteins, hepatic triglycerides and kidney lipids. Our analyses revealed that prebiotics alone induced a more significant reduction of triglycerides in the liver compared to synbiotics, and this was uncorrelated with changes in plasma lipoproteins. Collectively, these data indicate that probiotic and prebiotic modulations of gut microbiota affect different regulatory mechanisms of host energy and lipid metabolism at the level of absorption, mobilization and recirculation.

Conclusion

These studies exemplify the application of top-down systems biology[57] to capture the long-range effects of the gut microbiota modulation in various tissues and to assess the depth of symbiotic control in complex organisms. The nutritionally induced microbial changes modulated host lipid, carbohydrate and amino acid metabolism at a panorganismal scale. Altogether, our data highlight the contribution of microbial activity to dietary calorie recovery and to tightly regulate dietary fat absorption on one hand, lipid synthesis, circulation/recirculation and utilization by the host on the other hand. The observation that dietary modulations of gut microbial activity may lead to differential homocysteine or ascorbate metabolism, with inferred effects on glucose metabolism, insulin sensitivity, antioxidation or steroidogenesis is of particular interest. These studies suggest that major mammalian metabolic processes and interorgan cross-talks are strongly connected to the microbial activity, which in turn may have long-term health consequences to the host. In particular, our results further suggest that the gut microbiota should be a nutritional target for future interventions aiming to modulate host carbohydrate and lipid metabolism. Therefore, the integration of both individual metabolic predisposition and latent gut microbial metabolic contribution to the host will provide a future basis to develop optimized nutritional management.

Abbreviations: CFU, colony forming unit; GC, gas chromatography; HBM, human baby microbiota; ND, not detected; NMR, nuclear magnetic resonance; O-PLS-DA, orthogonal projection to latent structure discriminant analysis; PCA, principal component analysis; SD, standard deviation; SCFA, short chain fatty acid; STOCSY, statistical total correlation spectroscopy; TMA, trimethylamine, TMAO; trimethylamine-*N*-oxide.

Acknowledgment. This work received financial support from Nestlé to F.-P.M. and Y.W., and from the International Study of Macro/micronutrient and Blood Pressure grant 1-R01-HL084228−01A1 to I.K.S.Y. We acknowledge the help and input of Isabelle Rochat, Catherine Murset and Gloria Reuteler for microbial and short chain fatty acid profiling, Josette Sidoti and Francoise Delmas for preparation of *L. rhamnosus* biomass, Fabrizio Arigoni for making available microbiological resources, and Christian Darimont, Mathieu Membrez, Irina Monnard and Dominique Donnicola for measures of liver gene expression. We thank John Newell, Monique Julita, Massimo Marchesini, Catherine Schwartz and Christophe Maubert for provision of the animal facilities and expertise. We acknowledge the input of Marc-Emmanuel Dumas, Ziad Ramadan, Jean-Marc Aeschlimann and Cristina Legido-Quigley for statistical analysis and bile acid profiling techniques.

Supporting Information Available: Materials and Methods and Supplementary Table S1. This material is available free of charge via the Internet at http://pubs.acs.org.

References

(1) Ley, R. E.; Hamady, M.; Lozupone, C.; Turnbaugh, P. J.; Ramey, R. R.; Bircher, J. S.; Schlegel, M. L.; Tucker, T. A.; Schrenzel, M. D.; Knight, R.; Gordon, J. I. Evolution of mammals and their gut microbes. *Science* **2008**, *320* (5883), 1647–1651.

(2) Nicholson, J. K.; Holmes, E.; Wilson, I. D. Gut microorganisms, mammalian metabolism and personalized health care. *Nat. Rev. Microbiol.* **2005**, *3* (5), 431–438.

(3) Dethlefsen, L.; Fall-Ngai, M.; Relman, D. A. An ecological and evolutionary perspective on human-microbe mutualism and disease. *Nature* **2007**, *449* (7164), 811–818.
(4) Shanahan, F. The host-microbe interface within the gut. *Best Pract. Res. Clin. Gastroenterol.* **2002**, *16* (6), 915–931.
(5) Guigoz, Y.; Dore, J.; Schiffrin, E. J. The inflammatory status of old age can be nurtured from the intestinal environment. *Curr. Opin. Clin. Nutr. Metab. Care* **2008**, *11* (1), 13–20.
(6) Rawls, J. F.; Mahowald, M. A.; Ley, R. E.; Gordon, J. I. Reciprocal gut microbiota transplants from zebrafish and mice to germ-free recipients reveal host habitat selection. *Cell* **2006**, *127* (2), 423–433.
(7) Palmer, C.; Bik, E. M.; Digiulio, D. B.; Relman, D. A.; Brown, P. O. Development of the Human Infant Intestinal Microbiota. *PLoS Biol.* **2007**, *5* (7), e177.
(8) Kunz, C.; Rudloff, S.; Baier, W.; Klein, N.; Strobel, S. Oligosaccharides in human milk: structural, functional and metabolic aspects. *Annu. Rev. Nutr.* **2000**, *20*, 699–722.
(9) Penders, J.; Vink, C.; Driessen, C.; London, N.; Thijs, C.; Stobberingh, E. E. Quantification of Bifidobacterium spp., Escherichia coli and Clostridium difficile in faecal samples of breast-fed and formula-fed infants by real-time PCR. *FEMS Microbiol. Lett.* **2005**, *243* (1), 141–147.
(10) Parracho, H.; McCartney, A. L.; Gibson, G. R. Probiotics and prebiotics in infant nutrition. *Proc. Nutr. Soc.* **2007**, *66* (3), 405–411.
(11) Turnbaugh, P.; Ley, R.; Mahowald, M.; Magrini, V.; Mardis, E.; Gordon, J. An obesity-associated gut microbiome with increased capacity for energy harvest. *Nature* **2006**, *444*, 1027–1031.
(12) Dunne, C. Adaptation of bacteria to the intestinal niche: probiotics and gut disorder. *Inflamm. Bowel. Dis.* **2001**, *7* (2), 136–145.
(13) Martin, F. P.; Dumas, M. E.; Wang, Y.; Legido-Quigley, C.; Yap, I. K.; Tang, H.; Zirah, S.; Murphy, G. M.; Cloarec, O.; Lindon, J. C.; Sprenger, N.; Fay, L. B.; Kochhar, S.; van, B. P.; Holmes, E.; Nicholson, J. K. A top-down systems biology view of microbiome-mammalian metabolic interactions in a mouse model. *Mol. Syst. Biol.* **2007**, *3*, 112.
(14) Li, M.; Wang, B.; Zhang, M.; Rantalainen, M.; Wang, S.; Zhou, H.; Zhang, Y; Shen, J.; Pang, X.; Zhang, M.; Wei, H.; Chen, Y.; Lu, H.; Zuo, J.; Su, M.; Qiu, Y.; Jia, W.; Xiao, C.; Smith, L. M.; Yang, S.; Holmes, E.; Tang, H.; Zhao, G.; Nicholson, J. K.; Li, L.; Zhao, L. Symbiotic gut microbes modulate human metabolic phenotypes. *Proc. Natl. Acad. Sci. U.S.A.* **2008**, *105* (6), 2117–2122.
(15) Yap, I. K.; Li, J. V.; Saric, J.; Martin, F. P.; Davies, H.; Wang, Y.; Wilson, I. D.; Nicholson, J. K.; Utzinger, J.; Marchesi, J. R.; Holmes, E. Metabonomic and microbiological analysis of the dynamic effect of vancomycin-induced gut microbiota modification in the mouse. *J. Proteome Res.* **2008**, *7* (9), 3718–3728.
(16) Rezzi, S.; Ramadan, Z.; Martin, F. P.; Fay, L. B.; Bladeren, P. V.; Lindon, J. C.; Nicholson, J. K.; Kochhar, S. Human Metabolic Phenotypes Link Directly to Specific Dietary Preferences in Healthy Individuals. *J. Proteome Res.* **2007**, *6* (11), 4469–4477.
(17) Rezzi, S.; Ramadan, Z.; Fay, L. B.; Kochhar, S. Nutritional metabonomics: applications and perspectives. *J. Proteome Res.* **2007**, *6* (2), 513–525.
(18) Martin, F. P.; Wang, Y.; Sprenger, N.; Yap, I. K.; Lundstedt, T.; Lek, P.; Rezzi, S.; Ramadan, Z.; van, B. P.; Fay, L. B.; Kochhar, S.; Lindon, J. C.; Holmes, E.; Nicholson, J. K. Probiotic modulation of symbiotic gut microbial-host metabolic interactions in a humanized microbiome mouse model. *Mol. Syst. Biol.* **2008**, *4*, 157.
(19) Martin, F.-P. J.; Wang, Y.; Sprenger, N.; Yap, I. K. S.; Rezzi, S.; Ramadan, Z.; Pere-Trepat, E.; Rochat, F.; Cherbut, C.; van Bladeren, P.; Fay, L. B.; Kochhar, S.; Lindon, J. C.; Holmes, E.; Nicholson, J. K. Top-down Systems Biology Integration of Conditional Prebiotic Transgenomic Interactions in a Humanized Microbiome Mouse Model. *Mol. Syst. Biol.* **2008**, *4*, 205.
(20) Reeves, P. G.; Nielsen, F. H.; Fahey, G. C., Jr. AIN-93 purifieddiets for laboratory rodents: final report of the American Institute of Nutrition ad hoc writing committee on the reformulation of the AIN-76A rodent diet. *J. Nutr.* **1993**, *123* (11), 1939–1951.
(21) Amaretti, A.; Bernardi, T.; Tamburini, E.; Zanoni, S.; Lomma, M.; Matteuzzi, D.; Rossi, M. Kinetics and metabolism of Bifidobacterium adolescentis MB 239 growing on glucose, galactose, lactose, and galactooligosaccharides. *Appl. Environ. Microbiol.* **2007**, *73* (11), 3637–3644.
(22) Waters, N. J.; Garrod, S.; Farrant, R. D.; Haselden, J. N.; Connor, S. C.; Connelly, J.; Lindon, J. C.; Holmes, E.; Nicholson, J. K. High-Resolution Magic Angle Spinning 1H NMR Spectroscopy of intact Liver and Kidney: Optimisation of sample preparation procedures and biochemical stability of tissue during spectral acquisition. *Anal. Biochem.* **2000**, *282*, 16–23.
(23) Trygg, J.; Wold, S. O2-PLS, a two-block (X-Y) latent variable regression (LVR) method with an integrated OSC filter. *J. Chemom.* **2003**, *17*, 53–64.
(24) Cloarec, O.; Dumas, M. E.; Trygg, J.; Craig, A.; Barton, R. H.; Lindon, J. C.; Nicholson, J. K.; Holmes, E. Evaluation of the orthogonal projection on latent structure model limitations caused by chemical shift variability and improved visualization of biomarker changes in 1H NMR spectroscopic metabonomic studies. *Anal. Chem.* **2005**, *77* (2), 517–526.
(25) Cloarec, O.; Dumas, M. E.; Craig, A.; Barton, R. H.; Trygg, J.; Hudson, J.; Blancher, C.; Gauguier, D.; Lindon, J. C.; Holmes, E.; Nicholson, J. Statistical total correlation spectroscopy: an exploratory approach for latent biomarker identification from metabolic 1H NMR data sets. *Anal. Chem.* **2005**, *77* (5), 1282–1289.
(26) Folch, J.; Lees, M.; Sloan stanley, G. A simple method for the isolation and purification of total lipides from animal tissues. *J. Biol. Chem.* **1957**, *226* (1), 497–509.
(27) Nicholson, J. K.; Wilson, I. D. High resolution proton magnetic resonance spectroscopy of biological fluids. *Prog. Nucl. Magn. Reson. Spectrosc.* **1989**, *21* (4−5), 449–501.
(28) Wang, Y.; Bollard, M. E.; Keun, H.; Antti, H.; Beckonert, O.; Ebbels, T. M.; Lindon, J. C.; Holmes, E.; Tang, H.; Nicholson, J. K. Spectral editing and pattern recognition methods applied to high-resolution magic-angle spinning 1H nuclear magnetic resonance spectroscopy of liver tissues. *Anal. Biochem.* **2003**, *323* (1), 26–32.
(29) Martin, F. P.; Wang, Y.; Sprenger, N.; Holmes, E.; Lindon, J. C.; Kochhar, S.; Nicholson, J. K. Effects of Probiotic Lactobacillus Paracasei Treatment on the Host Gut Tissue Metabolic Profiles Probed via Magic-Angle-Spinning NMR Spectroscopy. *J. Proteome Res.* **2007**, *6* (4), 1471–1481.
(30) Gavaghan, C. L.; Holmes, E.; Lenz, E.; Wilson, I. D.; Nicholson, J. K. An NMR-based metabonomic approach to investigate the biochemical consequences of genetic strain differences: application to the C57BL10J and Alpk:ApfCD mouse. *FEBS Lett.* **2000**, *484* (3), 169–174.
(31) Macfarlane, S.; Macfarlane, G. T.; Cummings, J. H. Review article: prebiotics in the gastrointestinal tract. *Aliment. Pharmacol. Ther.* **2006**, *24* (5), 701–714.
(32) Kikuchi, H.; Andrieux, C.; Szylit, O. Effects of galacto-oligosaccharides on bacterial enzymatic activities and metabolite production in rats associated with a human flora. *Proc. Nutr. Soc.* **1992**, *51*, 7A.
(33) Rycroft, C. E.; Jones, M. R.; Gibson, G. R.; Rastall, R. A. A comparative in vitro evaluation of the fermentation properties of prebiotic oligosaccharides. *J. Appl. Microbiol.* **2001**, *91* (5), 878–887.
(34) Gibson, G. R.; Roberfroid, M. B. Dietary modulation of the human colonic microbiota: introducing the concept of prebiotics. *J. Nutr.* **1995**, *125* (6), 1401–1412.
(35) Tzortzis, G.; Goulas, A. K.; Gee, J. M.; Gibson, G. R. A novel galactooligosaccharide mixture increases the bifidobacterial population numbers in a continuous in vitro fermentation system and in the proximal colonic contents of pigs in vivo. *J. Nutr.* **2005**, *135* (7), 1726–1731.
(36) Niculescu, M. D.; Zeisel, S. H. Diet, methyl donors and DNA methylation: interactions between dietary folate, methionine and choline. *J. Nutr.* **2002**, *132* (8 Suppl), 2333S–2335S.
(37) Craig, S. A. Betaine in human nutrition. *Am. J. Clin. Nutr.* **2004**, *80* (3), 539–549.
(38) Olthof, M. R.; Brink, E. J.; Katan, M. B.; Verhoef, P. Choline supplemented as phosphatidylcholine decreases fasting and post-methionine-loading plasma homocysteine concentrations in healthy men. *Am. J. Clin. Nutr.* **2005**, *82* (1), 111–117.
(39) Finkelstein, J. D.; Martin, J. J.; Harris, B. J.; Kyle, W. E. Regulation of hepatic betaine-homocysteine methyltransferase by dietary betaine. *J. Nutr.* **1983**, *113* (3), 519–521.
(40) Wise, C. K.; Cooney, C. A.; Ali, S. F.; Poirier, L. A. Measuring S-adenosylmethionine in whole blood, red blood cells and cultured cells using a fast preparation method and high-performance liquid chromatography. *J. Chromatogr., B: Biomed. Sci. Appl.* **1997**, *696* (1), 145–152.
(41) Kliewer, S. A.; Sundseth, S. S.; Jones, S. A.; Brown, P. J.; Wisely, G. B.; Koble, C. S.; Devchand, P.; Wahli, W.; Willson, T. M.; Lenhard, J. M.; Lehmann, J. M. Fatty acids and eicosanoids regulate gene expression through direct interactions with peroxisome proliferator-activated receptors alpha and gamma. *Proc. Natl. Acad. Sci. U.S.A.* **1997**, *94* (9), 4318–4323.
(42) Bremer, J. Carnitine–metabolism and functions. *Physiol. Rev.* **1983**, *63* (4), 1420–1480.

(43) Delzenne, N. M.; Kok, N. Effect of non-digestible fermentable carbohydrates on hepatic fatty acid metabolism. *Biochem. Soc. Trans.* **1998**, *26* (2), 228–230.
(44) Kimura, H.; Fujii, H.; Suzuki, S.; Ono, T.; Arakawa, M.; Gejyo, F. Lipid-binding proteins in rat and human kidney. *Kidney Int. Suppl* **1999**, *71*, S159–S162.
(45) Moestrup, S. K.; Nielsen, L. B. The role of the kidney in lipid metabolism. *Curr. Opin. Lipidol.* **2005**, *16* (3), 301–306.
(46) Sparks, J.; Collins, H.; Chirieac, D.; Cianci, J.; Jokinen, J.; Sowden, M.; Galloway, C.; Sparks, C. Links Hepatic very-low-density lipoprotein and apolipoprotein B production are increased following in vivo induction of betaine-homocysteine S-methyltransferase. *Biochem. J.* **2006**, *15* (2), 363–371.
(47) Fernandez, M. L.; Vergara-Jimenez, M.; Conde, K.; bdel-Fattah, G. Dietary carbohydrate type and fat amount alter VLDL and LDL metabolism in guinea pigs. *J. Nutr.* **1996**, *126* (10), 2494–2504.
(48) McClenaghan, N. H. Physiological regulation of the pancreatic {beta}-cell: functional insights for understanding and therapy of diabetes. *Exp. Physiol.* **2007**, *92* (3), 481–496.
(49) Cani, P. D.; Neyrinck, A. M.; Fava, F.; Knauf, C.; Burcelin, R. G.; Tuohy, K. M.; Gibson, G. R.; Delzenne, N. M. Selective increases of bifidobacteria in gut microflora improve high-fat-diet-induced diabetes in mice through a mechanism associated with endotoxaemia. *Diabetologia* **2007**, *50* (11), 2374–2383.
(50) Cani, P. D.; Knauf, C.; Iglesias, M. A.; Drucker, D. J.; Delzenne, N. M.; Burcelin, R. Improvement of glucose tolerance and hepatic insulin sensitivity by oligofructose requires a functional glucagon-like peptide 1 receptor. *Diabetes* **2006**, *55* (5), 1484–1490.
(51) Redmann, A.; Mobius, K.; Hiller, H. H.; Oelkers, W.; Bahr, V. Ascorbate depletion prevents aldosterone stimulation by sodium deficiency in the guinea pig. *Eur. J. Endocrinol.* **1995**, *133* (4), 499–506.
(52) Patak, P.; Willenberg, H. S.; Bornstein, S. R. Vitamin C is an important cofactor for both adrenal cortex and adrenal medulla. *Endocr. Res.* **2004**, *30* (4), 871–875.
(53) Wu, X.; Iguchi, T.; Hirano, J.; Fujita, I.; Ueda, H.; Itoh, N.; Tanaka, K.; Nakanishi, T. Upregulation of sodium-dependent vitamin C transporter 2 expression in adrenals increases norepinephrine production and aggravates hyperlipidemia in mice with streptozotocin-induced diabetes. *Biochem. Pharmacol.* **2007**, *74* (7), 1020–1028.
(54) Hopkins, M. J.; Cummings, J. H.; McFarlane, G. T. Inter-species differences in maximum specific growth rates and cell yields of bifidobacteria cultured on oligosaccharides and other simple carbohydrate sources. *J. Appl. Microbiol.* **1998**, *85*, 381–386.
(55) Macfarlane, G. T.; Steed, H.; Macfarlane, S. Bacterial metabolism and health-related effects of galacto-oligosaccharides and other prebiotics. *J. Appl. Microbiol.* **2008**, *104* (2), 305–344.
(56) Schell, M. A.; Karmirantzou, M.; Snel, B.; Vilanova, D.; Berger, B.; Pessi, G.; Zwahlen, M. C.; Desiere, F.; Bork, P.; Delley, M.; Pridmore, R. D.; Arigoni, F. The genome sequence of Bifidobacterium longum reflects its adaptation to the human gastrointestinal tract. *Proc. Natl. Acad. Sci. U.S.A.* **2002**, *99* (22), 14422–14427.
(57) Nicholson, J. K. Global systems biology, personalized medicine and molecular epidemiology. *Mol. Syst. Biol.* **2006**, *2*, 52.

PR801068X